J Nanopart Res (2021) 23: 48
https://doi.org/10.1007/s11051-021-05156-x

REVIEW

Recent advances in polymer-coated iron oxide nanoparticles as magnetic resonance imaging contrast agents

Masoud Salehipour · Shahla Rezaei · Jafar Mosafer · Zahra Pakdin-Parizi · Ali Motaharian · Mehdi Mogharabi-Manzari

Received: 8 October 2020 / Accepted: 27 January 2021 / Published online: 15 February 2021

Abstract The surface–chemically modified superparamagnetic iron oxide nanoparticles are broadly investigated as magnetic resonance imaging contrast agents based on their unique characteristics such as high magnetization values, diameter from 4 to 100 nm, and narrow distribution of particle size. However, naked nanoparticles might be easily oxidized by the air leading to loss of dispersibility and magnetization. Therefore, suitable surface coating strategies were developed to increase the stability of magnetic iron oxide contrast agents in the physiological conditions. In addition, the polymer-coated agents possess an improved biocompatibility in comparison with conventional agents. This review discusses important aspects of newly developed magnetic contrast agents such as chemical synthesis strategies, physical parameters, relaxivity parameters, the effect of various coatings, and emerging applications. Disadvantages associated with commercially available gadolinium contrast agents are considered, and the advantages of potential applications of iron oxide alternatives to traditional agents are presented. Finally, perspectives of the future developments, applications, and concerns of the magnetic nanoparticles are also included.

Keywords Polymer-coated · Iron oxide nanoparticles · Magnetic resonance image · Contrast agent · Relaxivity

M. Salehipour
Department of Biology, Parand Branch, Islamic Azad University, Parand, Iran

S. Rezaei · M. Mogharabi-Manzari (✉)
Pharmaceutical Sciences Research Center, Hemoglobinopathy Institute, Mazandaran University of Medical Sciences, P.O. Box 48175-861, Sari 4847193698, Iran
e-mail: m.mogharabi@mazums.ac.ir

J. Mosafer
Research Center of Advanced Technologies in Medicine, Torbat Heydariyeh University of Medical Sciences, Torbat Heydariyeh, Iran

Z. Pakdin-Parizi
Department of Nuclear Medicine, Razavi Hospital, Mashhad, Iran

A. Motaharian
Food and Drugs Control Laboratory, Food and Drugs Administration, Birjand University of Medical Sciences, Birjand, Iran

Introduction

Magnetic resonance imaging (MRI) is widely used as an effective medical imaging technique providing both three-dimensional and cross-section images of soft tissues without using radioactive radiations. But the application of this technique is sometimes restricted by poor anatomic description and visualization of changes in soft tissues (Hao et al. 2010; Laurent et al. 2008). Therefore, paramagnetic contrast agents including dysprosium, gadolinium, and manganese complexes are used to raise the sensitivity of imaging (Xiao et al. 2016). Gadolinium is the most commonly used metal atom as an MRI contrast agent due to its most stable ion with unpaired electrons and high magnetic momentum (Caravan 2006). However, the sensitivity of

gadolinium-based contrast agents is still relatively low and a high dose of the agents may cause toxicity on some organs (Hermann et al. 2008). Some studies have reported the deposition of gadolinium in the bone and brain of patients with normal renal function, which raises concerns associated with the toxicity of gadolinium-based agents (Ramalho et al. 2016).

Over the past decade, the chemical synthesis methods and the applications of magnetic iron oxide nanoparticles have been widely studied for high-technology medical uses such as contrast agents in MRI, hyperthermia therapy, targeted drug or gene delivery, tissue engineering, and cell separation (Boyer et al. 2010). Magnetic iron oxide nanoparticle contrast agents might be considered as one of the most successful examples of medical applications of inorganic nanoparticles due to their unique properties such as effective contrast features, capability and flexibility of surface functionalization, and biocompatibility (Lee and Hyeon 2012; Santra et al. 2009).

After a while, iron was suggested as a potential contrast agent to overcome the mentioned disadvantages associated with applying gadolinium complexes. Iron is known as a vital element for several biological processes such as synthesis of heme applied in oxygen transport by hemoglobin and cellular respiration via iron-containing redox enzymes. Moreover, iron is a vital element in living organisms and plays a key role in metabolic pathways of the cells of all mammals (Abbate and Hider 2017; Coe et al. 2015). Although in recent years, magnetic nanoparticles have received considerable attention due to their unique potential applications as magnetic resonance contrast agents, naked nanoparticles might be easily oxidized by the air leading to loss of dispersibility and magnetization (Qiao et al. 2009). Therefore, by providing suitable surface coatings, some effective surface protection strategies were developed to increase the stability of magnetic iron oxide nanoparticles (Zheng et al. 2018). These approaches involve surface coating with some molecules such as biological molecules, surfactants, organic and inorganic polymers, and amino acids (Plachtova et al. 2018; Hedayati et al. 2018). Improved surface coating magnetic iron oxide nanoparticles with high relaxivity are developed to produce effective imaging contrast agents for prolonged circulation and specific targeted imaging, which offer unique opportunities for ultrasensitive magnetic resonance imaging and result in accurate diagnosis (Table 1) (Clauson et al. 2018; Wei et al. 2017).

This review summarizes the chemical synthesis approaches of magnetic iron oxide nanoparticles and their recent advances in biomedical imaging. In addition, it makes a bridge between synthetic and surface chemistry for the advancement of the potential applications of inorganic/organic-coated magnetic nanoparticles in magnetic resonance imaging.

MRI contrast agents

MRI technique

The first examination using the MRI technique on living human beings was performed in 1977, and since then, MRI has evolved into a widespread clinically important imaging tool (Hillman and Schwartz 1985). Magnetic resonance imaging is based on the behavior of hydrogen atoms in a magnetic field and is known as a very useful non-invasive diagnosing approach for internal organ imaging (Saddik et al. 2006).

The nucleus of an atom, with a net positive charge, consists of protons and neutrons. The nuclei of some elements have a specific property known as spin which is dependent on the number of protons or neutrons such as ^{1}H, ^{13}C, ^{31}P, ^{19}F, etc. The nuclei with an odd number of protons and/or neutrons possess quantized spin angular momentum and a magnetic moment (Liu et al. 1993). In the absence of an applied external magnetic field, all the spin states of the nucleus are in an equivalent level of energy with the same population. For example, hydrogen nuclei adopt only +1/2 or −1/2 spin and the nuclear magnetic moments (μ) in these two cases are pointed in opposite directions (Fig. 1).

The nuclear magnetic signal occurs when nuclei aligned with an external field are induced to absorb energy and change their spin orientation (Yang et al. 2004). The differences between the energy levels of these two spin states are dependent on the strength of the external magnetic field and increases with the raising of the field strength. Particular characteristics of hydrogen atoms in water molecules in the presence of magnetic fields provide a contrast between soft tissues according to their binding to water or lipid molecules (Henkelman et al. 2001).

In an applied magnetic field of 3 T, the energy difference of two spin states of a proton is compared with the radio frequency energy.

Table 1 Characteristics of FDA-approved iron oxide magnetic nanoparticle MRI contrast agents (Lohrke et al. 2016)

Generic name	Trade name	Developer	Core	Polymer	Core diameter (nm)	Iron concentration (mg ml^{-1})	Administration	Relaxivity (mM^{-1} s^{-1})		Approval year
								r1	r2	
Ferucarbotran	Resovist®	Bayer Healthcare	Fe^{2+}/Fe^{3+}	Carboxydextran	4.2	50	Injection	7	82	2001
Ferumoxides	Feridex® IV	Berlex Laboratories	Fe^{2+}/Fe^{3+}	Carboxydextran	4.9	11	Injection	22	53	2008
Ferumoxtran-10	Combidex®	AMAG Pharmaceuticals	Fe^{2+}	Carboxydextran	5.8	20	Injection	25	151	2007
NC100150	Clariscan®	Nycomed	Fe^{2+}/Fe^{3+}	Carbohydrate polyethylene glycol	6.4	30	Injection	21	35	2000
Ferumoxytol	Feraheme®	AMAG Pharmaceuticals	Fe^{2+}	Polyglucose sorbitol carboxymethyl ether	6.8	30	Injection	38	83	2009
Ferumoxsil	Gastromark™	Mallinckrodt Pharmaceuticals	Fe^{2+}/Fe^{3+}	Siloxane	8.3	52	Oral	3	72	1996

Magnetic fields in the range of 0.5–1.5 T are usually used in diagnostic MRI scanners, and 3-T systems are regularly used in research. High-field-strength systems possess some advantages including improved quantification, increased signal-to-noise ratio, enhanced temporal resolution, and reduced imaging time (Nielles-Vallespin et al. 2007). When the external magnetic field is applied, the nucleus begins to precess about its own axis of spin with angular Larmor frequency. The energy of radiofrequency waves of the oscillating electric field can be absorbed by other nuclei and changes the spin state (Grover et al. 2015).

The differences in signal intensity and resolution between tissues or anatomic spaces can be increased by the introduction of certain chemical agents for manipulating the relaxation parameters (longitudinal and transverse) of water as the most abundant molecule in human tissues.

T1- and T2-weighted MR imaging

The exited nuclei return to the ground state via longitudinal (spin-lattice) and transverse (spin-spin) relaxations that occur as first-order rate processes and are characterized by relaxation times T1 and T2, respectively (Mansfield et al. 1994). These two relaxation times are the fundamental parameters behind magnetic resonance imaging, and accurate determination of the T1 and T2 values allows quantitative imaging of tissues. Through the longitudinal relaxation process, the energy of the spins is transferred to the surroundings as thermal energy and increases the temperature of the matrix. The relaxation time T1 is also known as the time required for the z component of the magnetic field (M) to return to 63% of its original value and provides a mechanism by which the protons return to their original orientation (Fig. 2) (Plewes and Kucharczyk 2012). However, the inverse of the spin–lattice relaxation time (1/T1) is considered as the rate constant for the decay process.

On the other hand, the transverse relaxation process takes place in a plane perpendicular to the direction of the external magnetic field and does not change the energy of the spin system. The relaxation time T2 is the time required for the transverse component of M to decay to 37% of its initial value via irreversible processes (Nan et al. 2020).

A T1-weighted image is a basic pulse sequence in MRI and depicts differences in signal based on the intrinsic T1 relaxation time of various tissues. For example, fat shows high signal intensity on T1-weighted images, while fluid

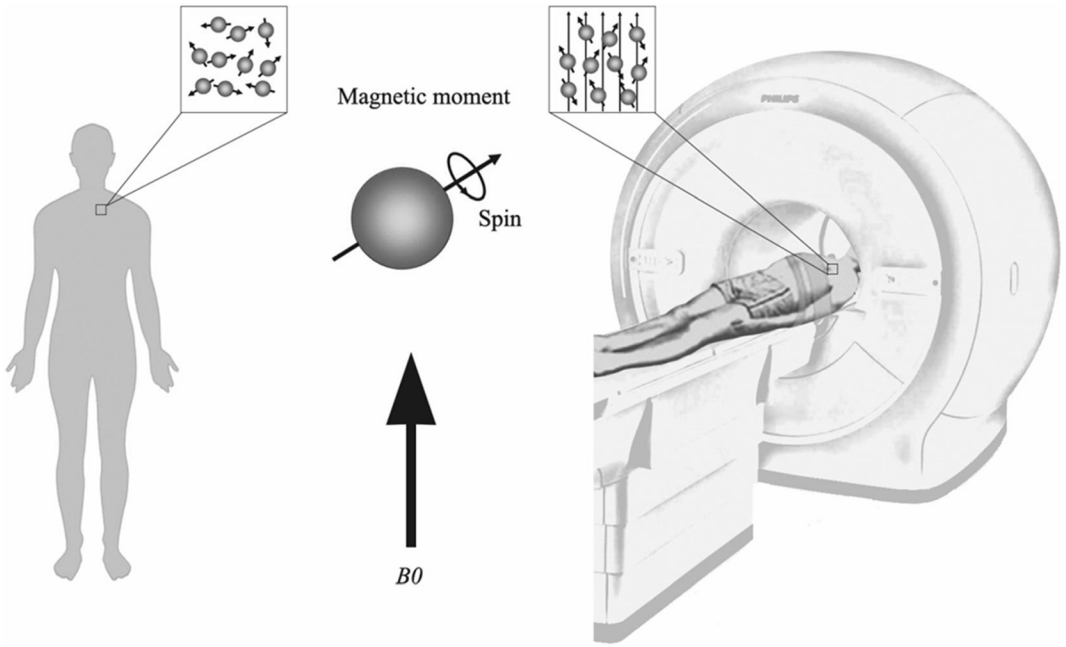

Fig. 1 Schematic representation of proton behavior in the presence of an external magnetic field applied in magnetic resonance imaging

reveals low signal intensity (Thomson et al. 1993). However, T2-weighted images provide the best depiction of disease, because most tissues involved in a pathologic process have higher water content than normal tissues such as cerebrospinal fluid and vitreous humor that appear bright on T2-weighted images (Hajela et al. 2000). The transverse relaxation in gradient-echo sequences (T2*) is a combination of T2 relaxation and relaxation caused by magnetic field inhomogeneities. The relationship between T2 and T2* can be expressed by the equation $1/T2^* = 1/T2 + \gamma\ \Delta B_{\text{inhom}}$, where γ is the gyromagnetic ratio and ΔB_{inhom} is the magnetic field inhomogeneity (Hajela et al. 2000).

Moreover, the resolution of MRI is increased by shortening the T1 and T2 relaxation times using contrast agents which increase the distinction between normal and affected tissues. Contrast agents are the essential elements of the developmental efforts to advance the medical diagnosis applications of MR technology.

Gadolinium-based contrast agents

Improvement of the signal intensity and the visibility of internal organs are the main purpose of using contrast agents that decrease the T1 relaxation of water molecules (Spandonis et al. 2004). Gadolinium (III)-containing chemical complexes are known as the most important applied contrast agents for raising the resolution of MRI. Gadolinium with seven unpaired electrons is a paramagnetic metal that behaves like protons in the presence of an external magnetic field. Stored energy in the processing electrons of gadolinium plays as a reservoir of magnetization, and this energy can be transferred to adjacent water protons helping them to reaccumulate longitudinal magnetization more quickly after an excitation pulse. This process eventually results in the shortening the T1 of adjacent protons leading to an increase in the signal intensity on T1-weighted images (Bonnet et al. 2010; Winter et al. 2011).

Gadopentetate dimeglumine (Magnevist®) was introduced in 1988 as one of the first developed contrast agents for clinical applications (Fig. 3). During the last decades, several gadolinium-containing agents were also approved worldwide for diagnostic imaging across the body including the heart, brain, breast, and lungs, and the circulatory, central nervous, genitourinary, gastrointestinal, lymphatic, and musculoskeletal systems (Lohrke et al. 2016).

Generally, gadolinium-based contrast agents are classified into four distinguished categories with different characteristics and important clinical implications, including linear, macrocyclic, ionic, and nonionic agents (Moser et al. 2018). Macrocyclic and ionic agents possess higher stability compared to linear and non-ionic

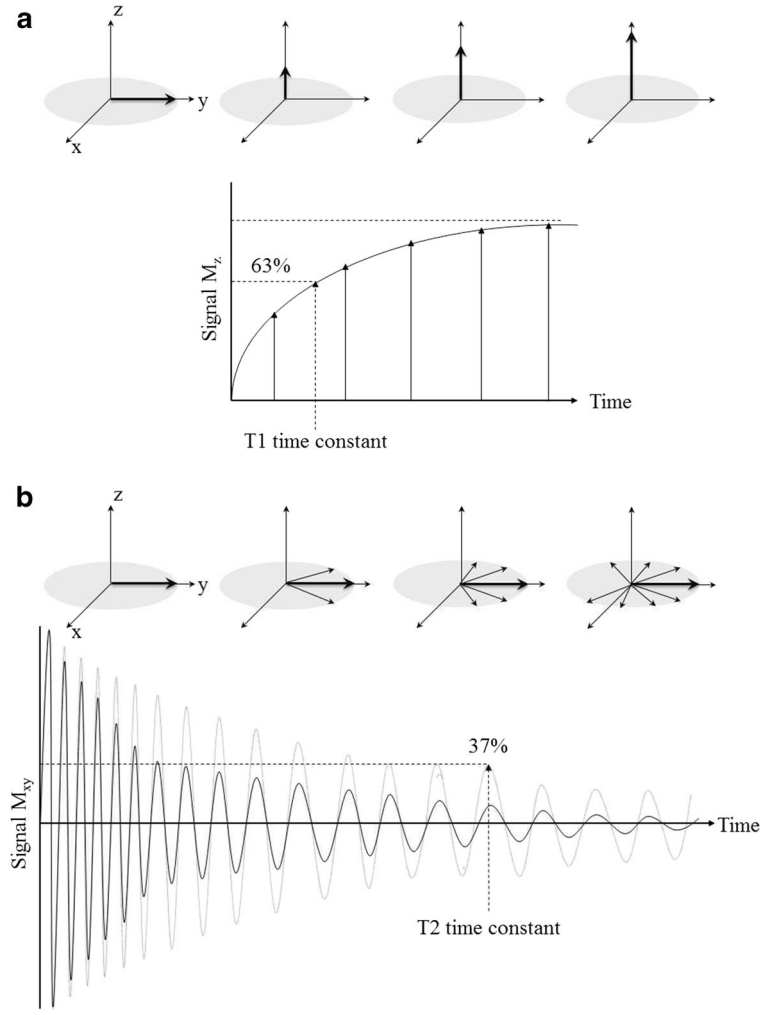

Fig. 2 The relaxation time of **a** longitudinal magnetization relaxation (T1) as the time required for longitudinal magnetization to recover to 63% of its maximum value and **b** transverse magnetization relaxation (T2) as the time required for transverse magnetization to fall to 37% of its initial value

compounds, respectively (Blahut et al. 2017). Gadoterate meglumine (Dotarem®), a thermodynamically stable MRI agent, consists of organic acid tetraxetan and is applied for visualization of the disruption of the blood–brain barrier and abnormal vascularity in the brain and spine (Kielar et al. 2018).

Although gadolinium complexes are the most potent contrast agents due to their unpaired electrons and isotropic electronic ground state, there are a few other metal ions such as Mn(II), Mn(III), Eu(II), and Fe(III) that can serve as effective relaxation agents.

Safety concerns of gadolinium complexes

Gadolinium chelates as extensively applied MRI contrast agents have conventionally been considered safe and well-tolerated when applied at recommended dosing levels (Rogosnitzky and Branch 2016). However, a correlation has been recognized between the administration of gadolinium-containing contrast agents and nephrogenic systemic fibrosis in patients with severe renal impairment (Berger et al. 2018; Fraum et al. 2017). Patients with normal renal function are able to remove the gadolinium complexes, while several reports in animals and humans have showed that Gd^{3+} is retained in some tissues (Blumfield et al. 2017). In addition, some in vitro studies revealed adverse effects of exposure or administration of gadolinium-containing contrast agents such as induction of apoptosis and necrosis in renal tubular cells (Rah et al. 2018). Moreover, significant growing data demonstrate the accumulation of gadolinium in the kidney, bone, and brain of patients exposed to gadolinium-containing MRI contrast agents (Behzadi et al. 2017; Dekkers et al. 2018; Prince and

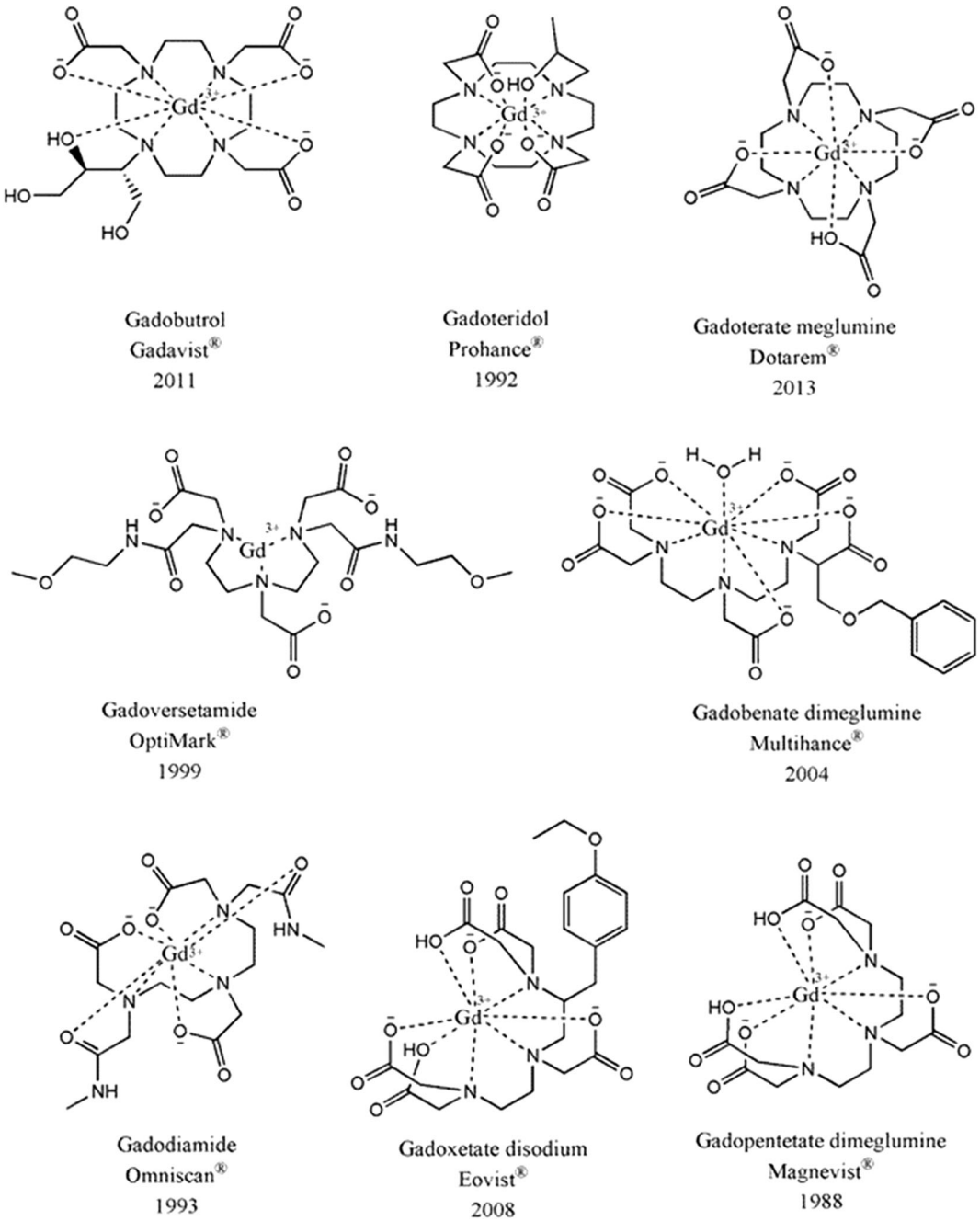

Fig. 3 The Food and Drug Administration (FDA)–approved gadolinium-based contrast agents (generic name, trade name, and approval year)

Weinreb 2018). Although early clinical investigations were primarily focused on gadolinium chelates, today, iron oxide nanocomposites have been identified as potential alternative MR contrast agents with higher T1 relaxivities and lower toxicity than gadolinium-containing agents.

Preparation methods of magnetic iron oxide nanoparticles

Several synthetic approaches are developed to produce magnetic iron oxide nanoparticles for medical imaging applications including co-precipitation (Fakayode et al.

2018; Mogharabi-Manzari et al. 2018a), microemulsions (Kaur et al. 2018), sol–gel syntheses (Sciancalepore et al. 2018), sonochemical reactions (Sodipo and Aziz 2018), and hydrothermal reactions (Lassoued et al. 2018). Generally, the synthesis of magnetic nanoparticles is known as a complicated process due to the colloidal nature of the particles. Adjustment of experimental conditions in the chemical approaches leads to the formation of monodisperse magnetic grains of appropriate size (Park et al. 2005). In addition, applying reproducible and simple procedures might be industrialized without the requirement of a complex, multistep, and expensive purification process such as magnetic filtration, ultracentrifugation, or size-exclusion chromatography (Teja and Koh 2009). However, some approaches have been developed to produce magnetic nanoparticles with homogeneous composition, narrow size distribution, and high magnetic saturation, such as co-precipitation, hydrothermal, sol–gel, and polyol methods (Fig. 4).

Co-precipitation

The co-precipitation approach is one of the most important chemical pathways for the synthesis of magnetic nanoparticles in which iron oxides are typically prepared by an aging process of a stoichiometric mixture of various ferric and ferrous salts in an aqueous solution (Kim et al. 2001; Lin et al. 2017). Thermodynamics of the co-precipitation method provide complete precipitation of magnetite at a pH ranging from 8 to 14 in the presence of a 2:1 stoichiometric ratio of Fe^{3+}/Fe^{2+} in a non-oxidizing environment (Lassoued et al. 2017; Mogharabi-Manzari et al. 2019a). However, one of the main advantages of this technique is the one-step production of large quantities of nanoparticles. In the co-precipitation approach, kinetic parameters control the growth of the crystal and limit the particle size distribution. The co-precipitation process consists of two main steps including nucleation and growth of the nuclei. The nucleation is a fast step and occurs when the concentration of the species reaches critical supersaturation, but growth of the nuclei is a slow process and performed by the diffusion of the solutes to the surface of the crystals (Suryawanshi et al. 2018). In a supersaturated solution, the nuclei form at the same time followed by their growth, resulting in a very narrow particle size distribution (Šutk et al. 2015; Mogharabi-Manzari et al. 2018b).

Extensive varieties of important factors affect the features of magnetic iron oxide nanoparticles such as size, magnetic characteristics, and surface properties (Kandasamy and Maity 2015; Mogharabi-Manzari et al. 2019b). The most important experimental conditions affecting the shape and the size of the nanoparticles are ionic strength and pH of the medium, temperature, type of the iron salts (chlorides, nitrates, perchlorates, or sulfates), and the molar ratio of Fe(II) to Fe(III) (Mahmed et al. 2014; Roth et al. 2015). Moreover, the control of the size can be achieved during the synthesis of magnetite nanoparticles using organic chelators such as acetate, citrate, or gluconate anions containing carboxylate or α-hydroxy carboxylate groups. In addition, some organic polymers are also applied for the coating of the surface of the nanoparticles leading to the control of their size and shape, such as polyvinyl alcohol, starch, dextran, and carboxydextran (Nadeem et al. 2016).

Temperature is a key factor in the synthesis of magnetic nanoparticles via co-precipitation process. At

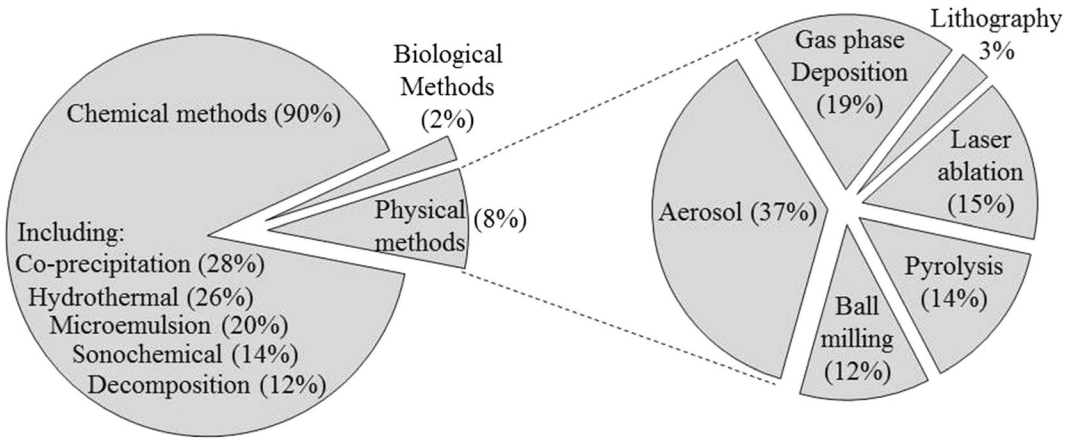

Fig. 4 Various methods used for production of iron oxide magnetic nanoparticles, extracted from 1560 papers published from 2000 to 2020

temperatures below 60 °C, the main product is Fe_2O_3, while Fe_3O_4 is the expected product when the reaction is carried out at temperatures above 80 °C. The nature of the alkali used in the synthesis procedure is also affected by the properties of the produced iron oxide nanoparticles, and it has been reported that replacing sodium hydroxide with ammonium hydroxide in the co-precipitation reaction improves the magnetization, crystallinity, and particle size (Mallakpour and Madani 2015).

Although the co-precipitation approach suffers from challenging control of shape and size distribution of the particles, this technique is still the preferred method for the synthesis of magnetic nanoparticles due to the convenient reaction conditions such as short reaction time, low temperatures used, and water as an environmentally friendly solvent, compared to hydrothermal and decomposition methods.

Hydrothermal

Hydrothermal reactions are carried out in aqueous media at temperatures and pressures higher than 200 °C and 2000 psi, respectively (Cheng et al. 2016; Gyergyek et al. 2017; Li et al. 2014). In the hydrothermal process, the characteristics of the prepared particles are affected by reaction conditions such as temperature, pressure, solvent system, and reaction time (Cui et al. 2006; Ozel et al. 2015). For example, the size of the precipitated iron oxide nanoparticles increases with the raising of water content of the solvent system as well as raising reaction time (Ge et al. 2009). Nucleation and grain growth are two key factors that mainly control the size of the particles in the hydrothermal process, and it was found that increasing the temperature and prolonging the reaction time might be favorable for crystal nucleation and growth, respectively (Takami et al. 2007). The hydrothermal approach possesses several advantages over the conventional methods, including the possibility of direct precipitation of crystallized nanoparticles from the solution that regulates the nucleation rate, uniformity, and growth rate (Table 2). However, advanced control of the processes of nucleation and growth improves the size and morphology of the produced magnetic nanoparticles and significantly reduces the aggregation of the nanoparticles (El-Boubbou 2018; Maghsodi et al. 2018).

The hydrothermal method is a very interesting technique for the production of iron oxide magnetic nanoparticles offering unique advantages such as short time reaction, controlled size and morphological characteristics, and high magnetization saturation.

Sol–gel reactions

Challenging control of the morphology of the nanoparticles in solid-state chemical synthesis reactions led to the development of some effective alternative wet methods (Gash et al. 2001). The sol–gel is an appropriate wet technique based on the hydroxylation and condensation of organic/inorganic molecular precursors for the production of nanostructured magnetic iron oxides in a solution (Lu et al. 2002). This technique consists of condensation and inorganic polymerization processes leading to the formation of a three-dimensional network of metal oxide (Akbar et al. 2015). Generally, the sol formation is performed by hydrolysis and partial condensation of precursors followed by gelation via a polycondensation process to form metal–oxygen–metal covalent bonds. Water acts as an oxygen supplier for the formation of metal oxide, and various metal salts are applied as the precursors of metals, such as acetates, alkaloids, citrates, chlorides, nitrates, or sulfates.

Some key factors are influencing the properties of the produced magnetic nanoparticles via sol–gel technique, including pH, temperature, precursor concentration, and solvent system (López-Ramón et al. 2018). In an aqueous sol–gel process, the control of size and morphology is complicated due to the high reactivity of metal precursors and dual activity of water as both a ligand and a solvent (Hussain et al. 2018). However, non-aqueous sol–gel systems were developed to overcome the disadvantages of aqueous solvents and offer improved crystallinity and uniform morphology. In the non-aqueous methods, the oxygen atom is provided by non-hydrolytic organic solvents such as alcohols, aldehydes, ethers, or ketones (Silva et al. 2017).

Polyol

The polyol technique is known as a useful method for the high yield synthesis of nano- and micro-sized particles with uniform morphology (Hachani et al. 2016). In this method, polyol compounds are employed as solvents, such as polyethylene glycol (PEG), 1,5-pentanediol, and 1,2-propylene glycol. Applying polyol solvents provides interesting properties such as high dielectric constants, ability

to dissolve various inorganic compounds, and high boiling points that offer an extensive operating temperature (Yamada et al. 2016). Polyols also act as reducing agents and stabilizers that prevent the aggregation of the nanoparticles and improve their size and morphology (Cheng et al. 2011). Generally, the synthesis of the nanoparticles via a polyol approach has four distinguished steps including metal precursor dissolution, intermediate formation, nucleation, and growth. In this method, metal salts are applied as starting compounds in combination with various anions such as Cl^-, SO_4^-, NO_3^-, and OH^- (Hachani et al. 2016). Increased solubility of precursors in the presence of polyols improves the formation of metal complexes. In the next step, the intermediate is precipitated and the metal clusters are formed via nucleation process. The efficiency of the nucleation step might be improved by adding external nanoparticles to the reaction mixture that facilitates the formation of fine and uniform particles (Yamada et al. 2016).

Although the growth process suffers from aggregation, long-chain alkylamines are used to adjust the shape and size of the nanoparticles as well as to prevent aggregation of the nanoparticles in the growth step (Cheng et al. 2011).

Miscellaneous methods

Flow injection is known as an important method for the continuous production of magnetic nanoparticles with uniform morphology and narrow size distribution (Salazar-Alvarez et al. 2006). However, in the flow injection approach, a particular design of the reactor can serve as an alternative to matrix confinement offering some unique advantages such as high homogeneity, high reproducibility, laminar conditions, and effective control of reaction conditions (Lunvongsa et al. 2006).

Aerosol approaches such as laser and spray pyrolysis have also become attractive based on continuous chemical processes that increase the rate of nanoparticle formation. In the spray pyrolysis method, a solution containing metal salts and reducing agent that is dissolved in an organic solvent are sprayed onto a hot surface to evaporate the solvent (Arimoto et al. 2002). Spray pyrolysis is a cost-effective technique that has some considerable benefits such as easy to perform under ambient conditions and no need for high-quality solvents and reagents. Furthermore, the characteristics of produced nanoparticles can be easily controlled by adjusting the reaction conditions including flow rate, concentrations of precursors, and temperature (Morales et al. 2003).

Laser pyrolysis as an effective approach for gas-phase synthesis of a wide range of nanoparticles performs based on decomposition of liquid or gas reactants using a powerful carbon dioxide laser followed by a quenching process (Bautista et al. 2005). In this process, the gaseous precursor is introduced into a reactor through an inert carrier gas and meets a high-power laser beam leading to molecular decomposition and vaporization to initiate nucleation and growth of nanoparticles with a narrow size distribution ranging from 5 to 60 nm (Rohani et al. 2019).

The sonochemical synthesis approach as one of the most important chemical synthesis techniques is widely applied for the preparation of ferrite nanoparticles with controllable physical characteristics such as morphology, particle size, and saturation magnetization (Yadav et al. 2020). Amorphous Fe_3O_4 nanoparticles are prepared using the sonolysis of an aqueous iron pentacarbonyl solution in the presence of sodium dodecyl sulfate (SDS) (Pinkas et al. 2008). The sonochemical synthesis of nanoparticles involves advantages such as high yield, reduced reaction time, and reduced costs (Mukh-Qasem and Gedanken 2005).

Coatings of iron oxide nanoparticles

Surface coatings are needed to improve the colloidal stability of the iron oxide magnetic nanoparticles in a physiological environment. Generally, the main purposes of surface modifications are improved dispersion of nanoparticles, adjustment of the surface activity, improvement of the mechanical and physicochemical characteristics, and increasing the biocompatibility of nanoparticles. Furthermore, the tendency of magnetic nanoparticles toward agglomeration can be prevented by coating of the surface with an organic or inorganic shell that enhances their hydrophilicity and biocompatibility (Dadfar et al. 2019).

Various synthetic and natural polymers are used for coating of iron oxide nanoparticles, such as porous and non-porous silica, PEG, poly(vinyl-pyrrolidone) (PVP), poly(vinyl alcohol) (PVA), poly(lactic-co-glycolic acid) (PLGA), gelatin, dextran, and chitosan (Table 3).

Table 2 Some advantages and disadvantages of the MOF synthesis methods

Method	Advantage	Disadvantage
Solvothermal	Good nucleation growth	Long reaction time
	High crystallinity	Organic solvent required
Mechanochemical	High efficiency	Low crystallinity
	Less solvent required	Decreased pore volume
Electrochemical	Mild reaction conditions	Low yield
	Short reaction time	Various structures
Continuous flow	Good porosity	Byproduct formation
	Controllable morphology	Difficult workup process

Silica

Magnetic iron oxide nanoparticles encapsulated in a suitable organic or inorganic shell have been successfully applied in an extensive variety of biomedical applications ranging from the separation of biological macromolecule to increasing the contrast of magnetic resonance images. Silica is one of the most commonly prepared and documented materials that is applied for coating the surface of various nanoparticles. Silica not only increases the stability of magnetic nanoparticles in both aqueous and organic solutions but also provides an appropriate support that can be easily functionalized through various functional groups (Fig. 5).

Nonporous silica coatings

Ultra-small and monodispersed magnetic Fe_3O_4 nanoparticles with a diameter of 4 nm were coated with silica shell using reverse microemulsion technique (Stepanov et al. 2018).

Iqbal et al. (Iqbal et al. 2015) applied superparamagnetic silica-coated iron oxide nanoparticles with T1 relaxivity of 1.2 mM^{-1} s^{-1} and low r_2/r_1 ratios 6.5 mM^{-1} s^{-1} as T1 contrast agents. In this study, T1-weighted magnetic resonance images were recorded using a clinical instrument. Accuracy of tumor diagnosis was improved using fluorescent silica-coated iron oxide nanoparticles (Jang et al. 2016). In addition, the silica-coated nanoparticles were used for in vitro cellular labeling and enhancement of contrast in MRI visualization (Raschzok et al. 2013).

Stepanov et al. (Stepanov et al. 2018) synthesized superparamagnetic iron-oxide nanoparticles via high-temperature decomposition of iron oleate as a precursor. In the next step, nanoparticles were coated with a silica layer to improve their hydrophilicity and prevent them from aggregation. They revealed transverse relaxivity values 134.74, 163.11, and 153.84 mM^{-1} s^{-1} for aqueous colloids at 0.47, 1.41, and 14.1 T, respectively. Moreover, the obtained nanoparticles showed r_1 and r_2 as 53.7 and 375.5 mM^{-1} s^{-1} at 15 MHz, respectively.

Synthesis of silica-coated contrast agents with a particle size of 10 nm showed that the coating process can also be applied for the production of the ultra-small contrast agent (Xue et al. 2014; Yan et al. 2004).

Zhang et al. (2007) showed that the T2 relaxivity of silica-coated particles (339.80 s^{-1} mM^{-1}) was higher than that of its derivatives such as (3-aminopropyl)trimethoxysilane-coated (134.40 s^{-1} mM^{-1}) and [N-(2-aminoethyl)-3 aminopropyl]trimethoxysilane-coated (84.79 s^{-1} mM^{-1}) particles. The obtained results revealed that silica-coated nanoparticles are very promising T1 contrast agent candidates with the extraordinary ability to increase the brightness of the images.

Porous silica coatings

Mesoporous silica-coated nanoparticles are recognized as safe and biocompatible materials for MRI cell labeling and tracking. Dispersion of paramagnetic iron species into highly porous silica was carried out successfully as a promising approach for the development of efficient T2-weighted MRI contrast agents applying in vivo cell tracking (Fig. 6) (Ye et al. 2012). The effect of surface coating on the efficiency of contrast agent was also studied, and it was found that the efficiency increased with the thickness of the coated nanoparticles (Ye et al. 2012).

Colloidal stability and minimal non-specific cell uptake of silica-coated contrast agents caused an enhancement in the MR signal. In addition, functionalized mesoporous silica coatings can improve MR imaging

Table 3 Physical, chemical, and biological properties of various iron oxide nanoparticles applied as MRI contrast agents

Coating polymer	Magnetization (emu g^{-1})	Core dimeter (nm)	Hydrodynamic diameter (nm)	Relaxivity parameter (mM^{-1} S^{-1})		MRI study		Cytotoxicity			Ref.
				R1	R2	Study type	Cells/organ	Cell	Concentration (μg/mL)	Viability (%)	
Mesoporous silica	20	180	150	–	192	In vitro	HeLa	L929	250	98	(Beg et al. 2017)
Mesoporous silica	–	58	80	6.9	–	In vitro	Lymph node carcinoma of prostate	Human skin fibroblasts	200	86	(Hurley et al. 2016)
Mesoporous silica	–	22	53	3.4	245	In vivo	Spleen	MCF-7 breast cancer	70	50	(Kim et al. 2007)
Mesoporous silica	48	50	60	4	84	In vitro	OC-k3	OC-k3	150	95	(Ye et al. 2012)
SiO_2	22.3	6.3	13.3	7.9	166.3	–	–	–	–	–	(Darbandi et al. 2013)
SiO_2	34.5	40	100	1.2	–	In vivo	–	HeLa	100	98	(Iqbal et al. 2015)
SiO_2	60	11	54	–	–	In vivo	SK-OV-3	SK-OV-3	20	83.5	(Jang et al. 2016)
SiO_2	–	1700	–		9.91	In vitro	HuH7	–	–	–	(Raschzok et al. 2013)
SiO_2	–	10	39		134	–	–	Human embryo lung	250	95	(Stepanov et al. 2018)
Mesoporous silica	–	46	95	–	288.7	In vivo	Liver	HEK293	5	96.2	(Xue et al. 2014)
SiO_2	20	10	220	–	–	In vivo	Brain	–	–	–	(Yan et al. 2004)
SiO_2	–	10	13	–	339.8	–	–	–	–	–	(Zhang et al. 2007)
Pegylated dendron	70	50	75	10	349	–	–	–	–	–	(Basly et al. 2010)
Oligoethyleneglycol–derivatized dendron	55	11	13.8	–	91	In vivo	Liver Kidney	Human tumor (U87 line)	2.3	94	(Basly et al. 2013)
Dextran dendrimer	65	8	–	–	39	In vitro	HeLa	–	–	–	(Bulte et al. 2001)
Poly(γ-glutamic acid) dendrimer	–	3.1	418.3	–	92.67	In vivo	Spleen	KB	100	100	(Cai et al. 2015)
Folic acid-PEG dendrimer	65	10	–	–	–	In vivo	B16 melanoma	MCF-7	10	92	(Chang et al. 2012a)
Dextran dendrimer	–	11	50	–	272	In vivo	–	U87	2.3	94	

Table 3 (continued)

Coating polymer	Magnetization (emu g^{-1})	Core dimeter (nm)	Hydrodynamic diameter (nm)	Relaxivity parameter (mM^{-1} S^{-1})		MRI study		Cytotoxicity			Ref.
				R1	R2	Study type	Cells/organ	Cell	Concentration (μg/mL)	Viability (%)	
											(Lamanna et al. 2011)
Folate dendrimer	–	11	78.8	–	192	In vitro	SKOV3	HeLa	150	96	(Luong et al. 2017)
Poly(amidoamine) dendrimer	–	8.4	–	–	78.8	In vitro	KB-HFAR	KB	100	100	(Shi et al. 2008a)
Poly(amidoamine) dendrimer	50	8.8	–	–	125	–	–	–	–	–	(Strable et al. 2001)
Poly(amidoamine) dendrimer	–	8.4	–	–	71.55	In vivo	–	–	–	–	(Sun et al. 2016)
Gelatin	41	7.8	178.2	–	153	In vivo	–	MCF-7	700	100	(Cheng et al. 2014)
Alginate	40	10	193.8	7.86	281.2	In vivo	–	–	–	–	(Ma et al. 2007)
Alginate	–	10	193.8	7.86	281.2	In vivo	Liver	–	–	–	(Ma et al. 2007)
Chitosan	57	17.2	–	–		–	–	–	–	–	(Haw et al. 2010)
Chitosan	17	10.78	128.4	9.44	64.31	In vivo	–	Skin fibroblast cells	2.60	80	(Sanjai et al. 2014)
Carboxymethyl chitosan	41.6	10	55.4	3.86	160.5	In vivo	Human mesenchymal stem	Human mesenchymal stem cells	50	80	(Shi et al. 2008b)
Chitosan	–	7.6	87.2	22	202.6	–	–	–	–	–	(Tsai et al. 2010)
Chitosan	–	–	90.8	–	140.93	In vivo	Lung	PC3	50	80%	(Wang et al. 2013)
Palmitoyl chitosan	14.4	–	136.6	–	139.9	In vivo	A549 xenograft tumors HeLa	L-O2	20	82.5	(Xiao et al. 2015)
Dextran	45	11	56	–	362	–	–	–	–	–	(Bautista et al. 2004)
Dextran	80	10	68	21	144	In vivo	SKBR-3	MCF-7	10	85	(Chen et al. 2009)
Dextran	–	9.1	24.9	–	161.3	In vivo	–	–	–	–	(Dai et al. 2014a)
Dextran	–	15	35.6	–	74	In vivo	–	Hep G2	10	90	(Naha et al. 2014)

Table 3 (continued)

Coating polymer	Magnetization (emu g^{-1})	Core dimeter (nm)	Hydrodynamic diameter (nm)	Relaxivity parameter (mM^{-1} S^{-1})		MRI study		Cytotoxicity			Ref.
				R1	R2	Study type	Cells/organ	Cell	Concentration (μg/mL)	Viability (%)	
Dextran	53.5	10	35	–	116	In vitro	Mice bearing MDA-MB-435 tumors	–	–	–	(Park et al. 2008)
Dextran	45.8	12	50	2.5	140.7	In vivo	Liver	Hep G2	50	82	(Saraswathy et al. 2014)
PVP	110	8	20	–	174.8	In vivo	Liver	–	–	–	(Lee et al. 2008)
PEG	47.9	10	77.0	–	155.3	In vivo	–	KB	200	85%	(Chen et al. 2010)
PEG	29.9	5	11.7	35.92	206.91	In vivo	Liver	NIH/3T3	192	67%	(Dai et al. 2014b)
PEG	0.03	–	95	–	178.6	In vivo	–	MDA-MB-435	100	100	(Gao et al. 2011)
PEG	–	6	20		38	In vivo	Kidney	–	–	–	(Gómez-Vallejo et al. 2018)
PEG	94	5.4	10.1	19.7	–	In vitro	HeLa	HeLa	125	90	(Hu et al. 2011)
PEG	–	12	25	0.84	92.7	In vivo	Brain	RAW 264.7	100	100	(Liu et al. 2014)
PEG-COOH	–	8	59.45	0.17	12.42	–	–	–	–	–	(Najafian et al. 2015)
PEG	40	20	–	–	6.96	–	–	Amniotic membrane stem	25	100	(Naseroleslami et al. 2016)
PEG	51	5.5	24	9.5	28.2	In vivo	Heart	–	–	–	(Sandiford et al. 2013)
PEG	48	11	145.8	–	123	In vivo	–	HeLa	100	91	(Thapa et al. 2017)
PEG	–	4	10	7.3	39	–	–	RAW 264.7	200	95	(Tromsdorf et al. 2009)
PLA-PEG	57.79	6	40	–	–	–	–	–	–	–	(Xiong et al. 2017)
PLGA	72.1	10	–	–	83.8	–	–	MCF-7	250	98	(Nkansah et al. 2011)
PLGA	49	7.5	141	–	289	–	–	–	–	–	(Pöselt et al. 2012a)
Polyglycerol	46.6	5.9	39	26.2	158.3	In vivo	Liver	–	–	–	

Table 3 (continued)

Coating polymer	Magnetization (emu g^{-1})	Core dimeter (nm)	Hydrodynamic diameter (nm)	Relaxivity parameter (mM^{-1} S^{-1})		MRI study		Cytotoxicity			Ref.
				R1	R2	Study type	Cells/organ	Cell	Concentration (μg/mL)	Viability (%)	
											(Arsalani et al. 2012)
Polyglycerol	–	11	30	25.3	74.8	In vitro	–	Human umbilical vein endothelial	100	50	(Nordmeyer et al. 2014)
Polyglycerol	30	9	27	6.64	64.2	In vitro	RAW macrophage	3T3 fibroblast	200	95	(Wang et al. 2009)
Polyvinylpyrrolidone	63	6.9	45	–	183.8	In vitro	Beta-TC-6	Beta-TC-6	100	95	(Huang et al. 2010)
Polyvinylpyrrolidone	–	37	100	–	248.89	In vivo	Liver	RAW 264.7	250	90	(Huang et al. 2010)
Polyvinylpyrrolidone	110	10	30	–	141.2	In vivo	–	–	–	–	(Lee et al. 2008)

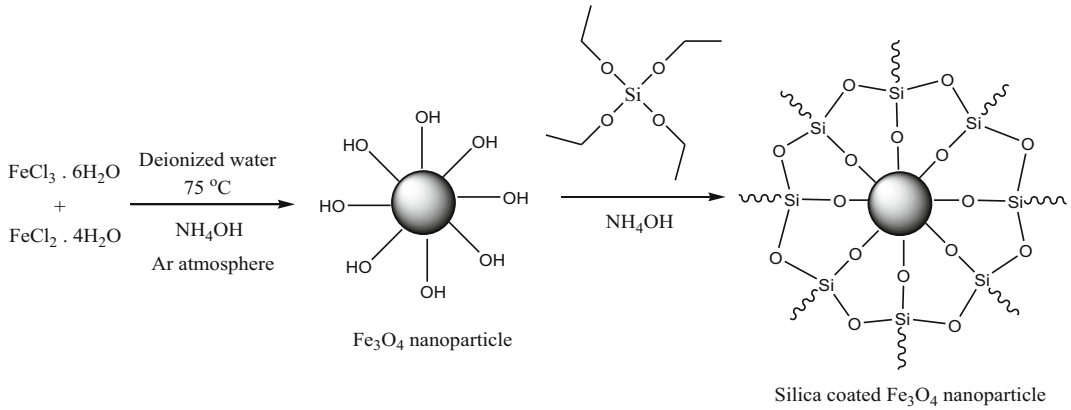

Fig. 5 Synthesis of silica-coated magnetic iron oxide nanoparticles

performance and increase the potential clinical applications of contrast agents (Hurley et al. 2016). Porous Fe_3O_4@SiO_2 nanorods with drug release capabilities were applied as magnetic resonance contrast agent (Beg et al. 2017). Patel et al. (2010) developed ion-sensing nanoparticles composed of a superparamagnetic iron oxide core and a porous silica shell with a great potential for use in MR cell tracking. Relaxivity of the prepared silica-coated nanoparticles was found to be 7.6 S^{-1} mM^{-1} that was comparable with the relaxivity of commercially available iron oxide contrast agents such as Feridex® (Patel et al. 2010). Chen et al. (2013) reported a monodisperse bifunctional silica system based on manganese-doped iron oxide nanoparticles as an MRI contrast agent. The nanoparticles with different iron to manganese ratios showed different saturation magnetizations and relaxivities. Magnetic resonance images of brain revealed an improvement in T1 values after intravenous injection of nanoparticles in rats (Chen et al. 2013). In addition, T2*-weighted images of liver showed a gradual darkening as time progressed. In the future, bifunctional silica-coated contrast agents might be applied for the clinical study of inactivated and silent areas of the brain.

Dendrimers

Dendrimers are repetitively branched macromolecules with unique molecular architectures and properties that make them attractive for biomedical applications such as detecting agents, affinity ligands, targeting components, imaging agents, and pharmaceutically active compounds (Basly et al. 2010; Qiao and Shi 2015). Generally, dendrimers can be divided into three distinguished domains including core, inner shells, and outer shell (Fig. 7) (Chang et al. 2012b). The core is normally a small molecule with a variable number of functional groups that define the number of branches in the final structure. Inner shells are composed of repeating units and define the generation (G). The outer shell possesses a large number of functional groups depending on the generation and can be manipulated to modulate dendrimer properties and applications (Sato et al. 2001). The dendrimer scaffolds have been used as powerful coatings in the development of different magnetic resonance imaging agents.

Dendrimers are not only used as stabilizers in the synthesis of iron oxide nanoparticles, they are also applied as coating for magnetic contrast agents. For

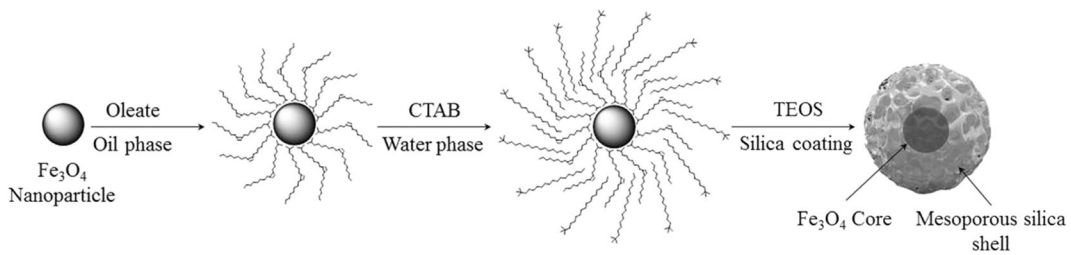

Fig. 6 Chemical procedure for the synthesis of mesoporous silica–coated iron oxide

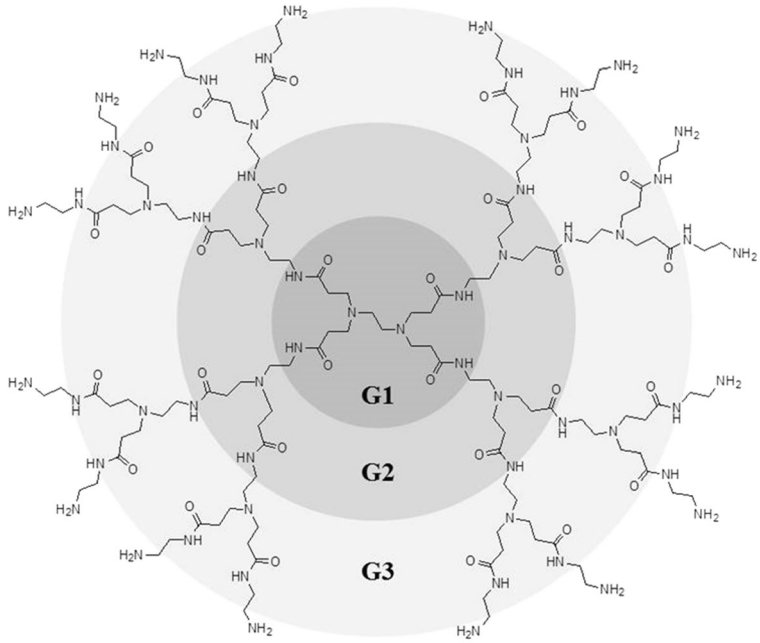

Fig. 7 Chemical structure of polyamidoamine dendrimer with three generations (G) as one of the most common classes of dendrimers suitable for the surface coating of iron oxide nanoparticles

example, Luong et al. (Luong et al. 2017) used a magnetic iron oxide core which was coated with folic acid–polyamidoamine dendrimers for delivery of 3,4-difluorobenzylidene-curcumin as a highly potent hydrophobic anticancer drug. The prepared particles were also studied as contrast agent, and the relaxation studies showed a significant decline in the T2-weighted signal intensity of the magnetic resonance images with increasing iron concentration (Luong et al. 2017).

An approach has been developed by combining a layer-by-layer self-assembly method and dendrimer chemistry to produce dendrimer-coated iron oxide nanoparticles for magnetic resonance imaging (Fig. 8). The fabricated nanoparticles were water-soluble, stable, and biocompatible. Folic acid–modified iron oxide nanoparticles have been efficiently applied as magnetic resonance imaging agents in both in vitro and in vivo studies (Shi et al. 2008b). To prepare these nanoparticles, Shi et al. (2008b) synthesized iron oxide nanoparticles with a diameter of 8.4 nm via controlled co-precipitation process, and the surface was modified with dendrimers composed of folic acid, fluorescein isothiocyanate, and polystyrene sulfonate sodium salt. These decorated nanoparticles were also used in resonance magnetic imaging of human epidermoid carcinoma cells where the T2 values were reduced as a function of iron concentration (Wang et al. 2007). In another study, Lamanna et al. (2011) reported iron oxide nanoparticles coated with small-size dendrons with a hydrodynamic diameter smaller than 100 nm. The prepared nanoparticles were applied in magnetic resonance and fluorescence imaging. Measurements of the relaxation at 1.5 T and 37 °C proved a relationship between iron concentration and the T1 value. Cai et al. (2015) developed a unique method to form folic acid–modified Fe_3O_4/Au nanocomposite as contrast agent for targeted dual-mode computed tomography and magnetic resonance imaging.

Dendrimers as promising coatings of magnetic contrast agents are a flourishing area of research mainly due to their precisely defined structure and composition, and also their high tunable surface chemistry (Basly et al. 2013). Reduction of the costs of dendrimer production is a major challenge for industrial development of dendrimer-based contrast agents.

In addition, the safety concerns of the dendrimer based nanoscale contrast agents is still raised because of the lack of total clearance of large molecules after administration and toxicity associated with some dendrimeric MR contrast agents. The improvement of multifunctional, multi-mode, and smart dendrimer-based contrast agents is an interesting research area and offer great challenges for development of potential clinical applications of dendrimer-based MRI contrast agents.

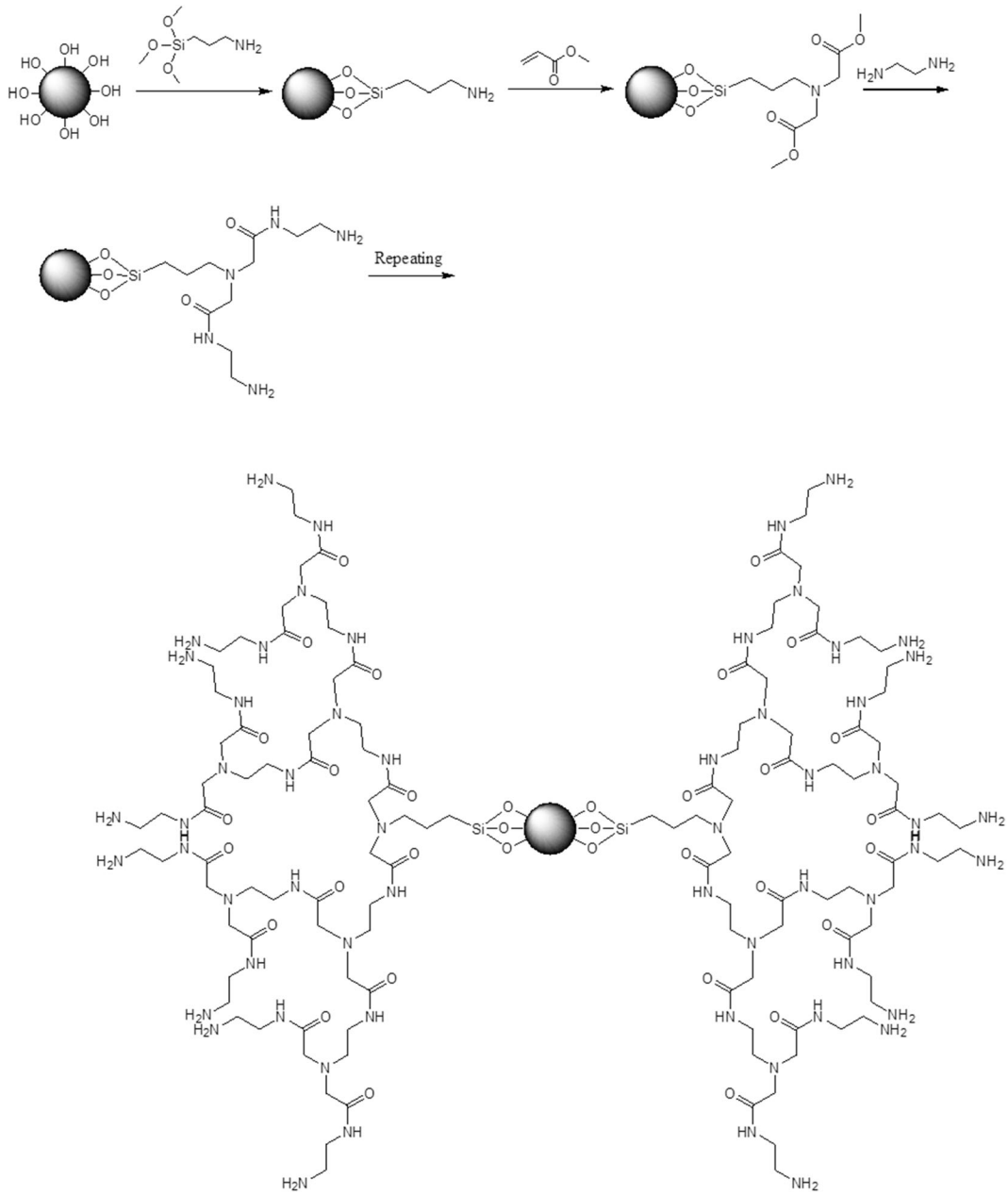

Fig. 8 Synthetic procedure for production of polyamidoamine-grafted iron oxide

Polymers

Natural polymers

Alginate and gelatin

Several natural polymers have been investigated for microencapsulation of iron oxide nanoparticles with appropriate biocompatibility and structural stability. Bar-Shir et al. (2014) reported the synthesis and the application of superparamagnetic iron oxide nanoparticles for the noninvasive determination of changes in extracellular calcium ion levels by conventional magnetic resonance imaging. They showed that coated nanoparticles with monodisperse and purified alginate could be successfully applied for the determination of Ca^{2+} concentrations in the range from 250 μM to 2.5 mM, even in the presence of various competitive ions

(Bar-Shir et al. 2014). Ma et al. (2008) synthesized alginate-coated superparamagnetic iron oxide contrast agents via a modified co-precipitation approach. The prepared particles possess T1 and T2 relaxivity values of 7.86 ± 0.20 mM^{-1} s^{-1} and 281.2 ± 26.4 mM^{-1} s^{-1} in saline at 1.5 T and 20 °C, respectively. In addition, the obtained results showed that alginate-coated superparamagnetic iron oxide nanoparticles might have the ability to improve the detection of liver tumors as an effective MR contrast agent. For example, it was found that incorporation of ferrofluid in alginate led to the successful synthesis of highly stable magnetic alginate nanocomposites (Ma et al. 2008; Shen et al. 2003).

Gelatin as a non-toxic, non-immunogenic, and biodegradable macromolecule is mainly obtained from the insoluble collagen of skin and bones via a hydrolysis process. Gelatins possess active groups such as acid, amine, and hydroxyl which made them attractive for biomedical applications. After injection of multifunctional gelatin-coated iron oxide nanoparticles, a darkening was observed at the tumor site and showed that the prepared particles can be used as T2-weighted MRI contrast agent (Cheng et al. 2014).

Chitosan

Chitosan-based MRI contrast agents have great potentials for the diagnosis of various diseases (Fig. 9). Xiao et al. (2015) reported magnetic MRI contrast agents coated by high molecular weight chitosan derivatives applying as a novel tumor-targeted vehicle. In this study, superparamagnetic iron oxide nanoparticles were encapsulated in self-aggregating polymeric folate-conjugated N-palmitoyl chitosan micelles (Fig. 10). After intravenous administration of the prepared micelles, the signal intensities of T2-weighted images in HeLa-derived tumors declined. Therefore, it was found that the produced magnetic micelles can potentially serve as effective and safe contrast agents for detecting folate receptor overexpressing tumors (Xiao et al. 2015). Iron oxide nanoparticles coated with chitosan-functionalized graphene oxide sheets have been also developed as MRI contrast agents. Wang et al. (2013)

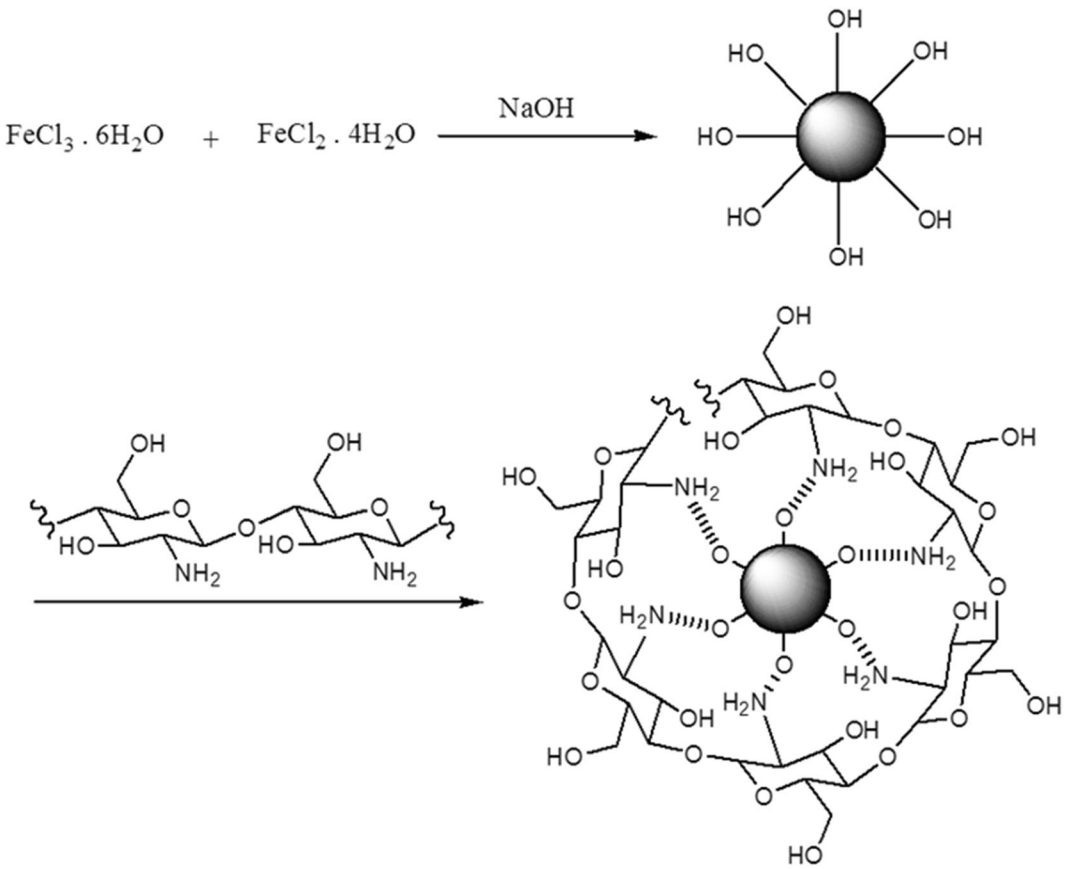

Fig. 9 Chitosan-coated magnetic iron oxide nanoparticles used as MRI contrast agent

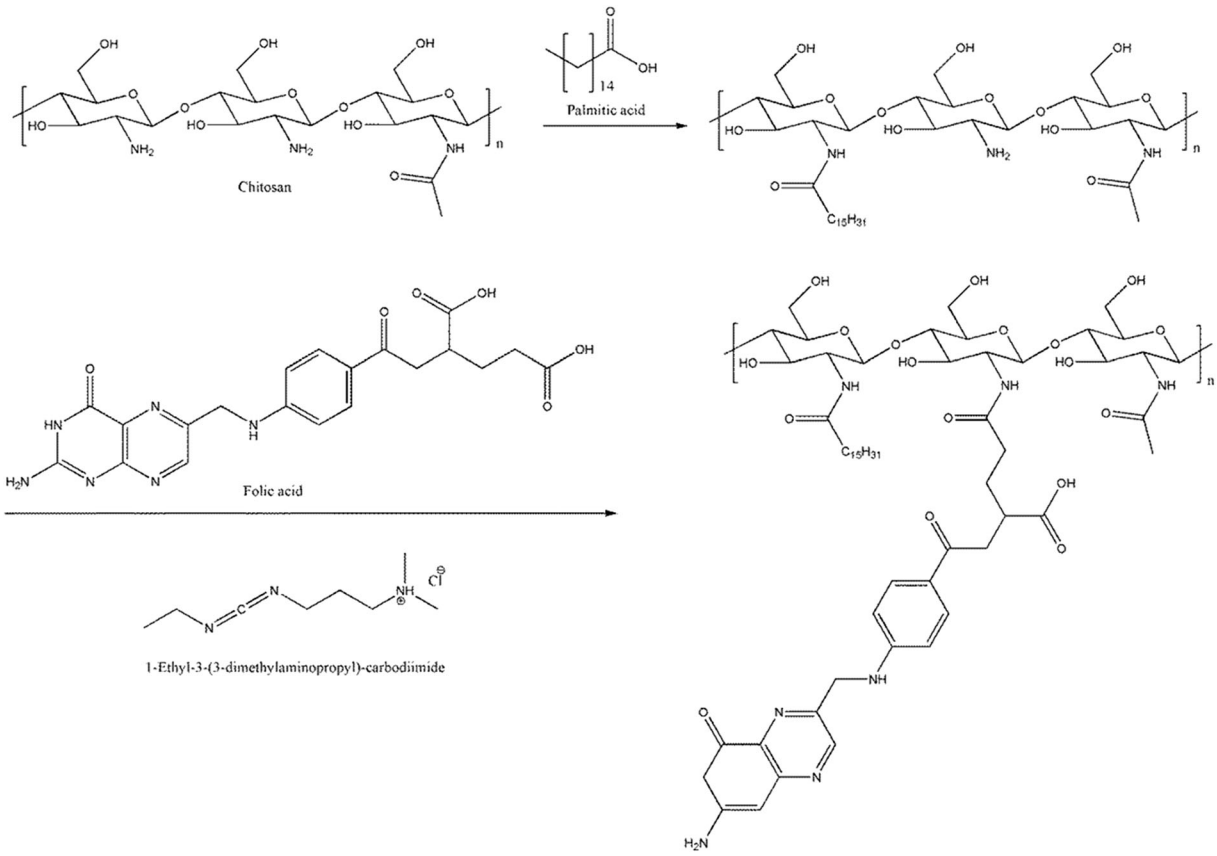

Fig. 10 Synthesis of folate-conjugated N-palmitoyl chitosan for coating of superparamagnetic iron oxide nanoparticles as MRI contrast agent

obtained the R2 relaxivity of 140.93 mM^{-1} S^{-1} for chitosan-coated iron oxide which proves that the prepared particles have sufficient magnetism to be effective as an MRI contrast agent.

Chitosan-coated superparamagnetic iron oxide nanoparticles were also used as a novel MRI contrast agent to monitor mouse islet grafts (Juang et al. 2010). Iron oxide microspheres coated by chitosan were also applied as contrast agent that improves the T2 value in the MRI process (Kim et al. 2007). The iron oxide nanoparticles directly were co-precipitated inside a porous matrix of chitosan in an aqueous solution at pH 9.5 and 50 °C. the obtained composite was applied as MRI contrast agent for cell tracking, and quantitative parameters obtained for R1, R2, and R2/R1 ratio were found to be as 22.0 mM^{-1} s^{-1}, 202.6 mM^{-1} s^{-1}, and 9.2, respectively (Tsai et al. 2010).

Polymer-stabilized iron oxide nanoparticles have been employed as MRI contrast agents due to their unique superparamagnetic properties. Shen et al. (2011) synthesized a quaternized chitosan, i.e., N-[(2-hydroxy-3-trimethylammonium)propyl] chitosan chloride, encapsulating superparamagnetic iron oxide that exhibited low toxicity, the least effect on cell growth, and improved relaxation processes resulting in an enhanced image contrast (Shen et al. 2011).

Several stem cell labeling approaches have been developed for detecting of fast growing and promising field of stem cell imaging by MRI. Many of them use iron oxide nanoparticles for cell labeling which provide improved signal effects on T2-weighted MR images. For example, in vivo tracking of mesenchymal stem cells labeled with a chitosan-coated superparamagnetic iron oxide nanoparticles using MRI was reported by Reddy et al. (Reddy et al. 2010). The ionotropic gelation method for the encapsulation of superparamagnetic iron oxide nanoparticles was reported and encapsulated nanoparticles showed enhanced dispersion ability in aqueous solution with R2/R1 ratios between 6.65–6.81 (Sanjai et al. 2014). In addition, Shi et al. (2008b) developed carboxymethyl chitosan-modified superparamagnetic iron oxide nanoparticles for magnetic

resonance imaging of stem cells with R1 and R2 values of 3.86 and 160.5 mM^{-1} s^{-1}, respectively. A value of R2/R1 ratio was calculated to be about 40 which is greater than those of some commercial agents such as Feridex and Resovist (between 7 and 17). Colloids of iron oxide nanoparticles dispersed in chitosan, in addition to improving the T2 value, also showed low toxicity and high intolerability when tested on New Zealand white rabbits (Lee et al. 2005). The prepared MRI contrast agents could potentially be applied in medical diagnostic methods and would provide noninvasive visualization by the improvement of T2 value.

Dextran

Colloidal suspensions of magnetic iron oxide nanoparticles were synthesized by Bautista et al. (2004) via the laser pyrolysis approach and were coated with dextran in an aqueous solution for rising biocompatibility of the nanoparticles. Studies have been performed on the synthesis of Herceptin-containing MRI contrast agents in which the surfaces of superparamagnetic iron oxide nanoparticles were coated with dextran and Herceptin to improve their physical and chemical properties such as magnetization, dispersion, and targeting of the specific receptors on cells. The prepared Herceptin-containing agents have been administered intravenously to mice bearing breast tumor allograft (Fig. 11). The MRI investigations have shown a high level of accumulation of the contrast agent within the tumor sites and prove the efficient targeting of cancer cells using dextran and Herceptin-containing contrast agent (Morales et al. 2003; Chen et al. 2009).

Dextran-coated magnetite nanoparticles were prepared by Bulte et al. (1992) for applying as an MRI contrast agent to visualize lesions with a blood–brain barrier disruption. Moreover, Dai et al. (2014a) used dextran-conjugated folic acid-coated iron oxide nanoparticles as MRI contrast agents for diagnosis and treatment response of rheumatoid arthritis. The T2 relaxation coefficient ($r2$) of the prepared nanoparticles was obtained by measuring the relaxation rate based on iron concentration as 161.3 mM^{-1} s^{-1}. Dextran-coated iron oxide magnetic nanoparticles were also prepared and applied as a potential contrast agent for MR imaging of lymph, bone marrow, and liver (Hong et al. 2008).

Naha et al. (2014) reported hybrid contrast agents composed of dextran-coated bismuth–iron oxide nanoparticles applied for MR imaging and computed tomography. T2-weighted MRI contrast decreased with increasing bismuth content, and the T2 relaxivity of the bismuth (30%) and iron (50%) formulation was found to be 0.4 mM^{-1} s^{-1} (Naha et al. 2014). In addition, Park et al. (2008) found that the geometry and the size of the iron oxide nanoparticles influence their efficiency by increasing the relaxivity in both in vitro and in vivo conditions. Increasing the ability of the nanoparticles to attach to tumor cells was caused by enhanced multivalent interactions between peptide modified particles and target cell receptors. Dextran-stabilized superparamagnetic iron oxide nanoparticles were also applied for in vivo MR imaging of liver fibrosis, and the evaluation of magnetic relaxivity on a 1.5 T showed R2/R1 ratio of 56.28 (Saraswathy et al. 2014).

Synthetic polymers

Polyethylene glycol

Polymer-coated contrast agents are of special interest due to their intrinsic advantages including excellent biocompatibility, low toxicity, long-term stability, and facile conjugation with functional molecules. For example, the most successful strategy to minimize aggregation is to coat the nanoparticles' surface with hydrophilic polymers such as polyethylene glycol (PEG). Monodisperse iron oxide nanoparticles coated with PEG at various molecular weights were prepared by Chen et al. (2010) via the self-assembly process and as an MRI contrast agent were applied for in vitro cellular uptake studies. The obtained results showed that the saturation magnetization and T2 relaxivity decreased when coating thickness increased (Chen et al. 2010). Dai et al., (2014b) prepare PEG-coated superparamagnetic iron oxide nanoparticles with an average hydrodynamic diameter of 11.7 nm via a facile one-pot approach and examined the synthesized nanoparticle as an MRI contrast agent. The nanoparticles were characterized in terms of their magnetic resonance imaging properties and the dual contrast in both T1- and T2-weighted MR imaging significantly improved with longitudinal and transverse relaxivity of 35.92 mM^{-1} s^{-1} and 206.91 mM^{-1} s^{-1}, respectively.

Several pH-responsive polymeric micelles with a capability of rapid responding to an acidic stimuli environment were prepared by Gao et al. (2011) and applied as intelligent carriers to deliver iron oxide nanoparticles

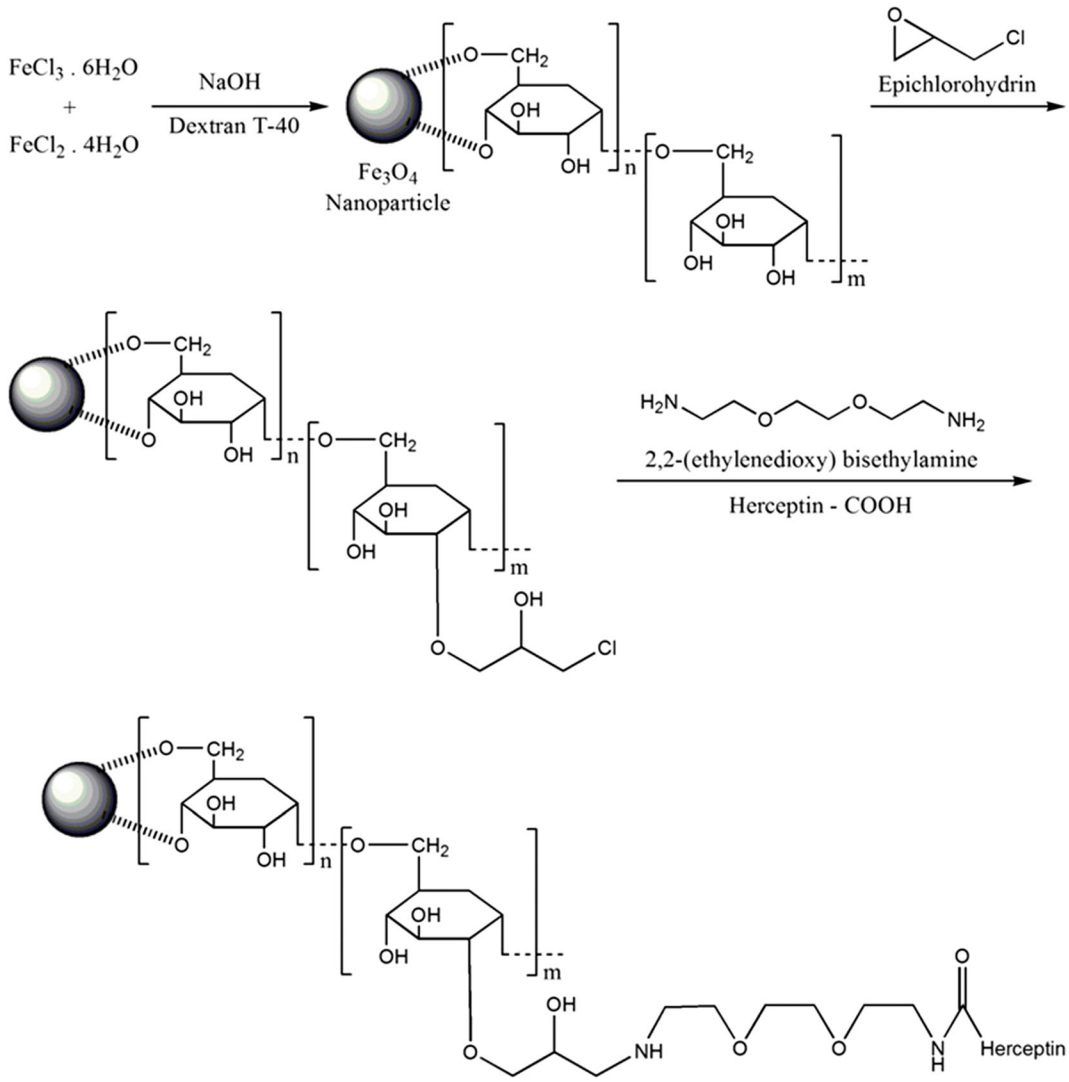

Fig. 11 Synthetic procedure of Herceptin–dextran iron oxide nanoparticles

for MRI. In their study, iron oxide nanoparticles were encapsulated in the polymeric micelles and used as MRI contrast agents by introducing amidoamine groups into the pH-sensitive poly(β-amino ester) blocks (Fig. 12). In this structure, methoxy poly(ethylene glycol) and poly(β-amino ester)/(amidoamine) moieties of the micelle act as a hydrophilic shell and pH-sensitive component, respectively (Gao et al. 2011).

An efficient and facile approach was developed for the synthesis of ultra-small PEGylated iron oxide nanoparticles acting as dual contrast agents for T1- and T2-weighted MRI with high crystallinity and size uniformity with an average diameter of 5.4 nm (Hu et al. 2011). The investigation of PEGylated iron oxide nanoparticles revealed a remarkable saturation magnetization, R1, and R2/R1 ratio as 94 emu g^{-1}, 19.7 mM^{-1} s^{-1}, and 2.0, respectively (Hu et al. 2011). Iron oxide nanoparticles coated with poly(ethylene glycol)-poly(aspartic acid) block copolymer were also synthesized as unique MR contrast agents for in vivo imaging of tumors (Kumagai et al. 2007).

Lutz et al. (2006) reported the synthesis of a polymeric composite containing polyethylene glycol and methacrylic acid via the central radical polymerization approach (Fig. 13). The prepared poly(oligo(ethylene glycol) methacrylate-co-methacrylic acid) composite was used as a coating for magnetic iron oxide nanoparticles and tested as an MRI contrast agent. The diameter of the magnetic nanoparticles was adjusted in the range

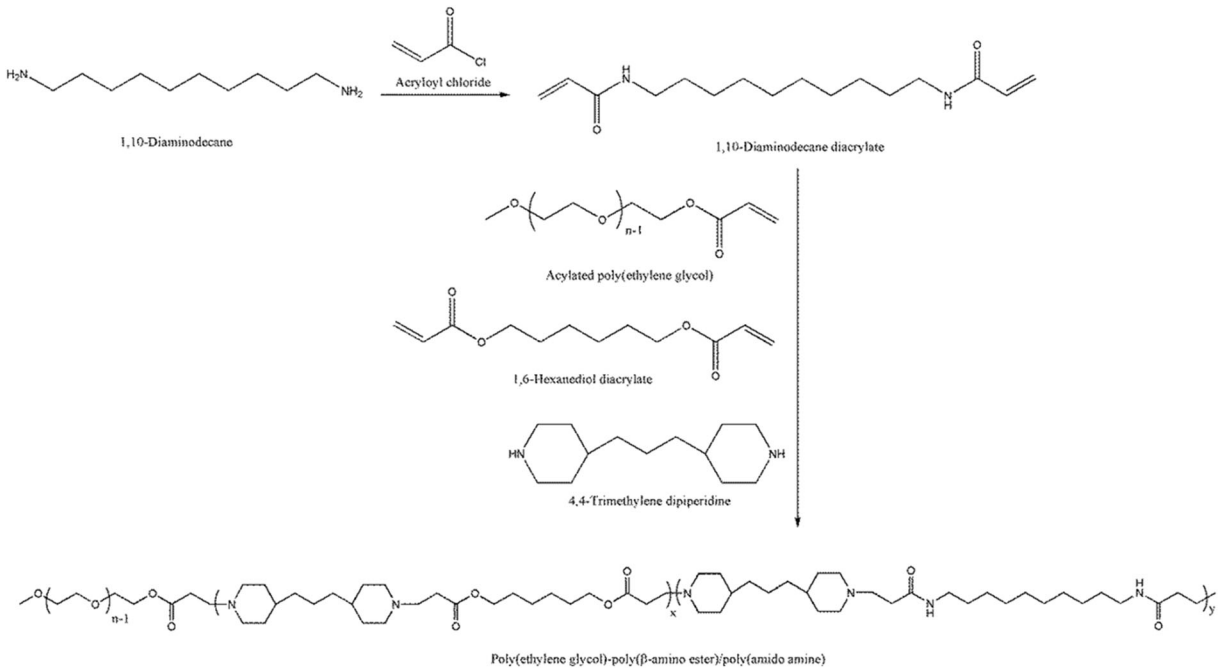

Fig. 12 PEG-poly(β-amino ester)/(amido amine) composite as coating of magnetic nanoparticles applied as contrast agent

of 10 to 25 nm by changing the initial coating polymers concentration (Lutz et al. 2006).

The prepared nanoparticles exhibited high colloidal stability in both aqueous solutions and physiological buffers. However, maximum liver accumulation was observed 6 h after intravenous administration in rats, indicating a prolonged circulation time for the polymer-coated nanoparticles compared to commercial agents such as Resovist®, which accumulate in the liver only 5 min after administration (Lutz et al. 2006; Masoudi et al. 2012). However, the biodistribution kinetics of these promising PEGylated ultrasmall nanoparticles is currently an attractive research area.

Liu et al. (2014) applied PEGylated iron oxide nanoparticles for MRI of post-ischemic blood–brain barrier damages. The R2 value of PEG-coated particles was calculated to be 92.7 mM^{-1} s^{-1}. However, the intensity of the signal was increased in the presence of the PEGylated super magnetic iron oxide nanoparticles so that the R1 value was 0.84 mM^{-1} s^{-1} (Liu et al. 2014).

Ultra-small superparamagnetic iron oxide nanoparticles represent a promising platform for the development of agents for multimodal medical imaging. Sandiford et al. (2013) reported ultra-small superparamagnetic iron oxide nanoparticles coated by PEG polymer conjugate containing a terminal 1,1-bisphosphate group (Fig. 14). They found that the PEGylated nanoparticles were very stable in physiological solutions and possessed a longitudinal relaxivity of 9.5 mM^{-1} s^{-1}. The MR images and pharmacokinetic profile confirm the majority circulation of PEGylated nanoparticles in the bloodstream the high signal in the heart, blood vessels, and vascular organs. It

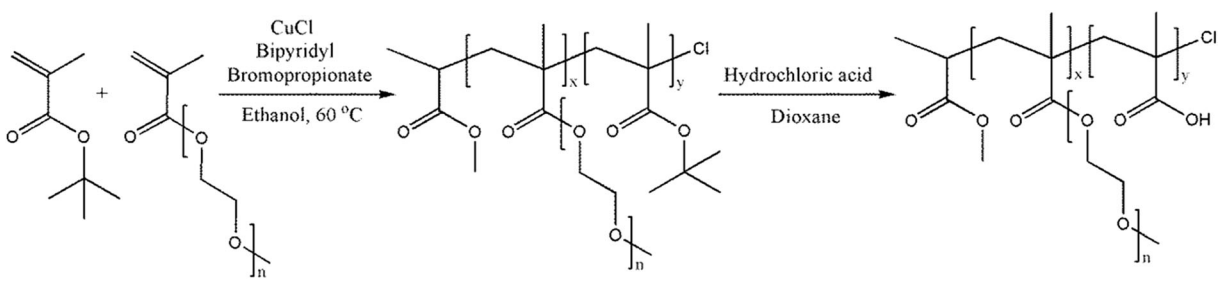

Fig. 13 Synthesis of a polymeric composite containing poly ethylene glycol and methacrylic acid via central radical polymerization approach

is expected that contrast agent based on PEG-coated iron oxide particles could provide better detectability and quantification capabilities of vascular targets involved in cardiovascular and oncologic diseases.

Pöelt et al. (2012b) reported detailed experimental data on contrast optimization of PEGylated iron oxide MR contrast agent with controlled aggregation of nanoparticles into stable and biocompatible clusters with narrow size distributions (Pöselt et al. 2012b). Superparamagnetic iron oxide nanoparticles with a diameter of 11 nm were PEGylated without anchoring groups and investigated as an efficient T2 contrast agent with a spin–spin relaxivity of $123 \pm 6\ mM^{-1}\ s^{-1}$ (Thapa et al. 2017).

It is essential to modify the surface of iron oxide nanoparticles with hydrophilic molecules that minimizes aggregation of the particles and prevents nonspecific uptake by mononuclear phagocyte system in physiological conditions. Therefore, PEGylation have been widely employed to modify the surface of the particles to enhance their function in physiological conditions. For example, the stability of PEG-oleic acid-coated magnetic nanoparticles was investigated under physiological conditions with various ionic strength and pH (Fig. 15). The obtained results showed that Fe_3O_4@PEG–oleic acid nanoparticles were highly stable in saline solution (up to 300 mM NaCl) and in the pH range of 3–10 (Yue-Jian et al. 2010).

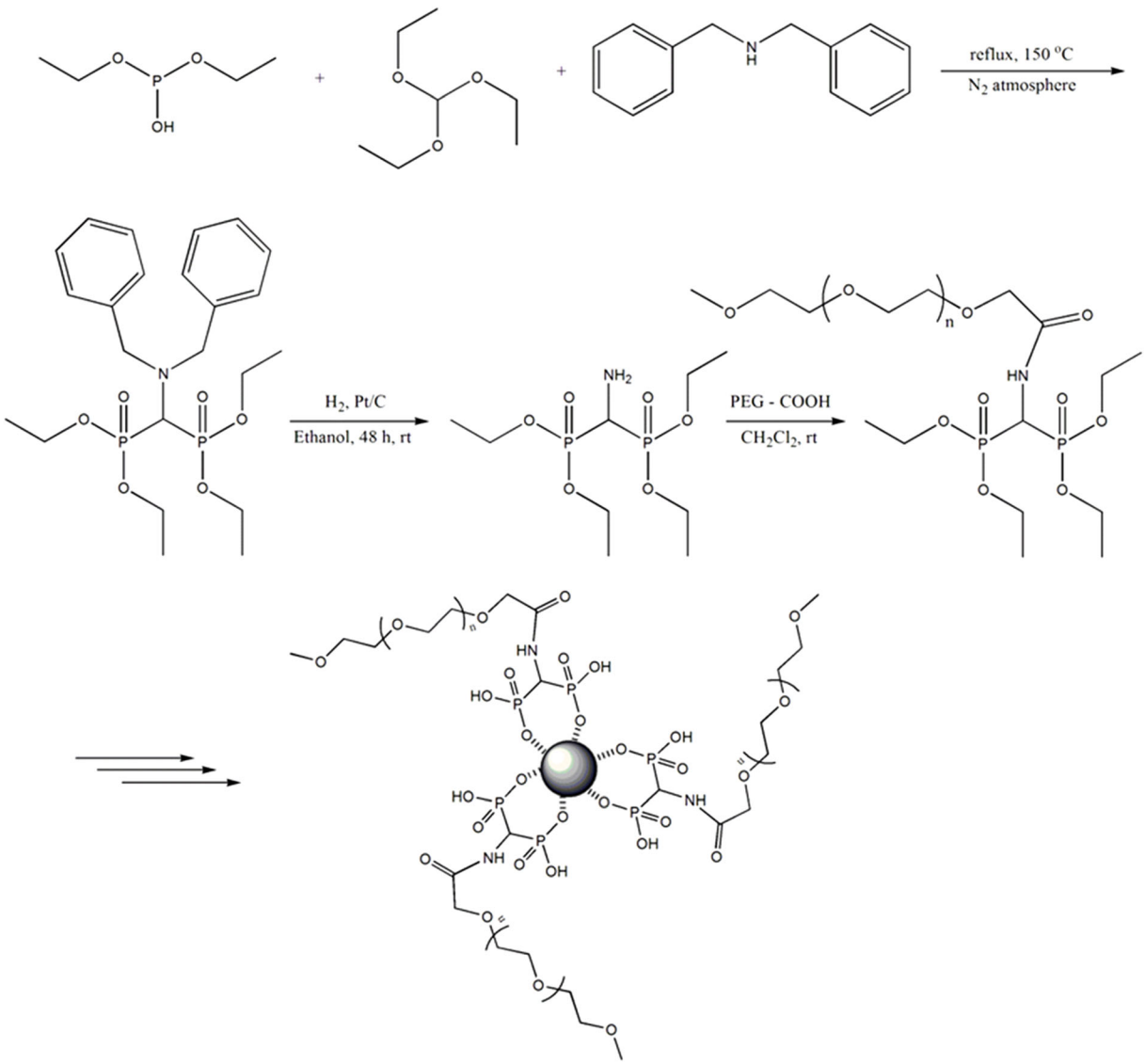

Fig. 14 Ultra-small superparamagnetic iron oxide nanoparticles coated by PEG polymer–conjugated 1,1-bisphosphate group

Using PEG in the synthesis of nanoparticles and coating of them combine the advantages of precipitation and thermal decomposition with hydrophilic nature for the control of size and geometry. In addition, PEG coating can decorate contrast agents with unique advantages such as nanoparticles with biocompatibility, hydrophilicity, soft surface, and in vivo long circulation.

Poly (lactic-co-glycolic acid)

Organic poly(lactic-co-glycolic acid) (PLGA)–coated nanoparticles have been widely applied in the various biomedical applications such as drug delivery, tissue engineering, and molecular imaging. Combining the advantages of PLGA microcapsules and magnetic Fe_3O_4 nanoparticles, the hybrid composites provide broader and feasible MRI contrast agents.

Superparamagnetic PLGA-coated iron oxide microspheres have been synthesized and applied as contrast agent in MRI of liver tissue with an improved T2-weighted signal (Zhou et al. 2015). Xu et al. (2015) developed a premix membrane emulsification technique to obtain uniform PEGylated PLGA microcapsules with magnetic iron oxide nanoparticles surrounded by a shell of polymer for magnetic resonance imaging. In vitro and in vivo studies showed that Fe_3O_4@PEG-PLGA microcapsules with a diameter about 3.7 μm and very narrow size distribution could efficiently act as a dual-modal contrast agent to simultaneously enhance ultrasound and magnetic resonance imaging performances (Xu et al. 2015). Multimodal and multifunctional contrast agents are considered as cutting edge technologies that develop the advantages of nanoparticles.

A cyclic peptide composed of arginine, glycine, and aspartate has been used for surface modification of PLGA-coated iron oxide nanoparticles as an MR contrast agent for the detection of thrombosis (Liu et al. 2017). The obtained results by Liu et al. (2017) demonstrated that the T2 signal reduced at the mural thrombus within 10 min after injection and then gradually increased until 50 min.

Polyvinylpyrrolidone

To improve the stability of Fe_3O_4 nanoparticles, a polymeric layer is coated on the surface of magnetic nanoparticles such as dendrimers, gelatin, dextran, chitosan, pullulan, PEG, and PLGA. Polyvinylpyrrolidone (PVP) attracted much interest in biomedical and molecular imaging because of biodegradability, non-toxicity, low cost, and antiviral properties.

Iron oxide nanoparticles coated by PVP have been used to investigate the influence of nanoparticle size on in vivo MRI of hepatic lesions. Huang et al. (2010) prepared the polymer-coated biocompatible nanoparticles with different sizes by a simple one-pot pyrolysis process. High T2 relaxivities and good crystallinity were observed in PVP-coated magnetic nanoparticles. In

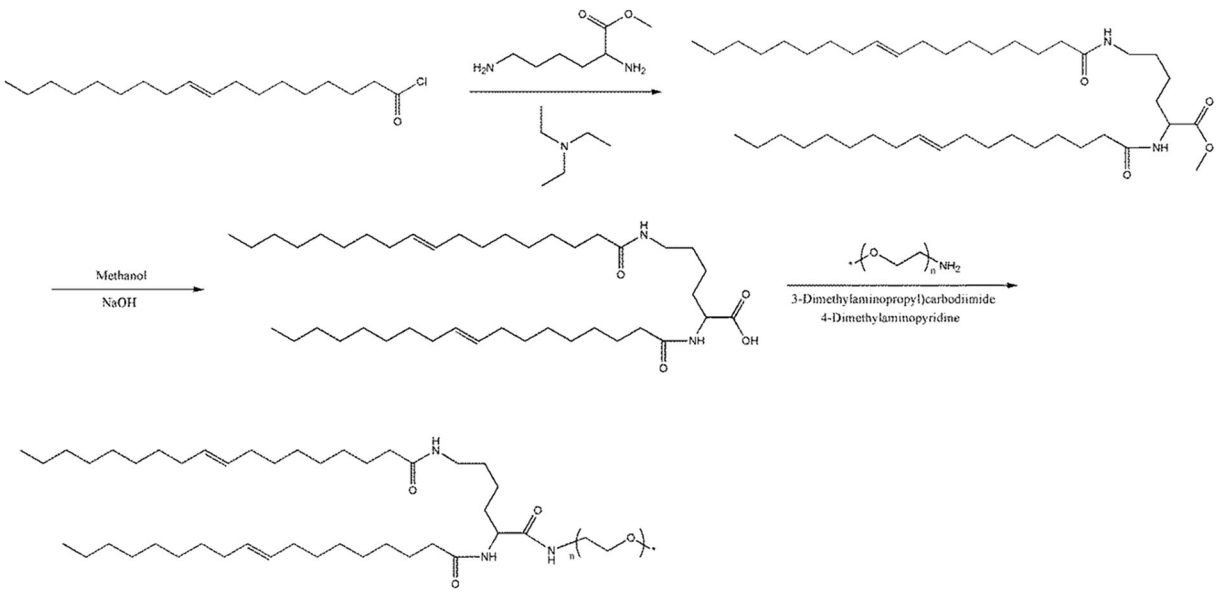

Fig. 15 Chemical synthetic procedure for the production of PEG-oleic acid as coating of iron oxide magnetic nanoparticles

addition, PVP was used as a stabilizer in the preparation of ultra-small Fe_3O_4 nanoparticles through the co-precipitation method (Zhang et al. 2010). The PVP-coated magnetic nanoparticles with a diameter between 6.5 and 1.9 nm were guided to the target sites using a permanent magnet. The particles were successfully concentrated, and an improved contrast was observed on the target area.

Lee et al. (2008) reported PVP-coated iron oxide nanoparticles as an MRI contrast agent with a core size of about 8–10 nm, the overall hydrodynamic diameter around 20–30 nm, and R2 and R1 relaxivity of 141.2 and 338.1 mM^{-1} s^{-1}, respectively. Water-soluble iron oxide nanoparticles coated with polyvinylpyrrolidone were also produced by transferring oleic acid-coated iron oxide nanocrystals from hexane to water (Li et al. 2015). The prepared nanoparticles showed excellent monodispersity with a particle size of about 14 nm and were guided to the target site by an external magnet. Therefore, the PVP-coated iron oxide particles encourage potential applications in MRI and magnetic delivery of contrast agents to the target organ.

Polyglycerol

The polyether backbone of polyglycerol is a water-soluble and biocompatible polymer that makes it an attractive polymeric compound for pharmaceutical and biomedical applications. The hyper-branched structure of the polyglycerol provides many reactive hydroxyl groups for modifications intended for various applications. In addition, the polyglycerol can be covalently grafted to the surface of superparamagnetic iron oxide nanoparticles. In this process, the surface of superparamagnetic magnetic iron oxide nanoparticles synthesized by co-precipitation method in aqueous solution is modified to introduce reactive groups. In the next step, polyglycerol is grafted on the surface of the activated nanoparticles by anionic ring-opening polymerization of glycidol in the presence of n-butyllithium as an initiator.

Arsalani et al. (Arsalani et al. 2012) examined the potential of a polyglycerol-coated ferrofluid for applying as a negative MRI contrast agent by studying its physical characteristics such as relaxometry and magnetometry (Fig. 16).

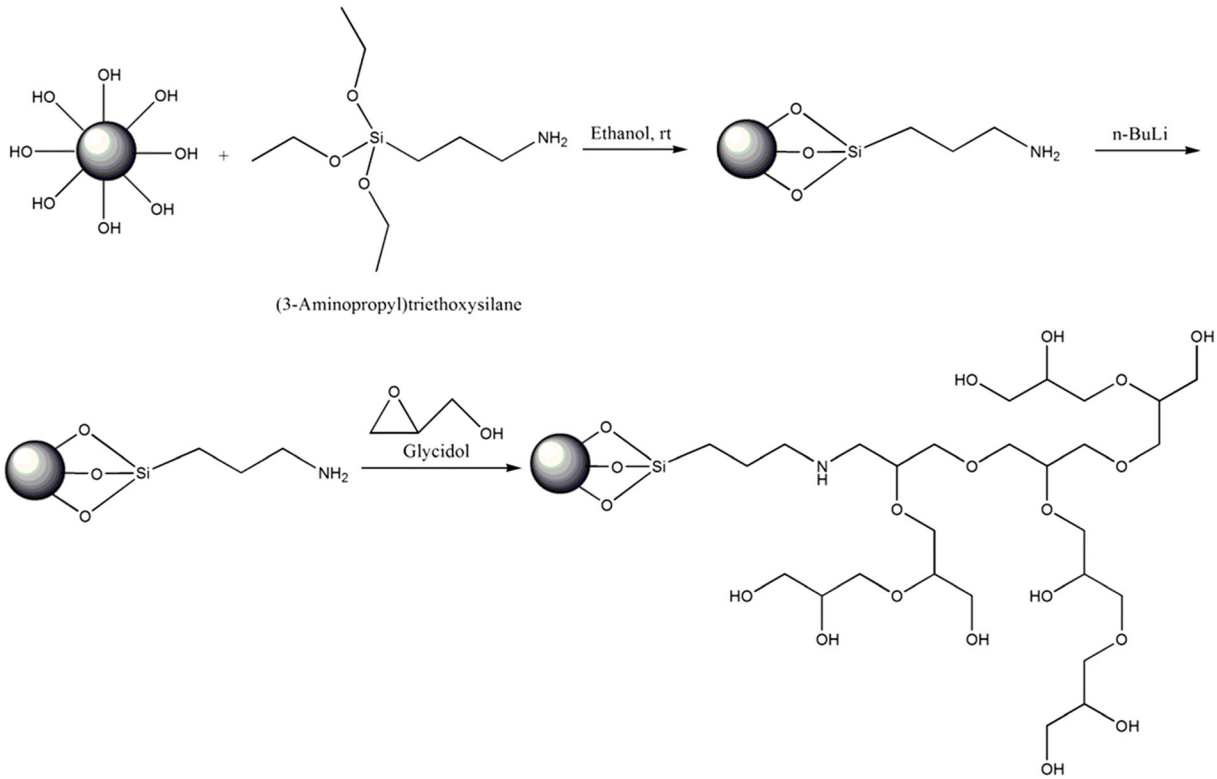

Fig. 16 Chemical synthesis approach for production of polyglycerol-coated superparamagnetic iron oxide nanoparticles

The obtained results showed that the calculated R1 and R2 at various magnetic fields were higher than those of some reported commercially available agents. In addition, in vivo MRI studies showed that the intravenously injected particles produced a modified contrast in the liver and kidneys that remained for 80 min and 110 min, respectively. The reduction of negative MR signals in the kidneys and liver over time suggested that polyglycerol coating optimized the renal excretion of the nanoparticles (Arsalani et al. 2012). Dendritic polyglycerol-modified iron oxide nanoparticles have been also reported as selective MRI contrast agents in which polyglycerol ligands are efficiently functionalized by one to three phosphonate groups acting as linkers (Nordmeyer et al. 2014). Although the high initial R2 value of the iron oxide nanoparticles usually decreases during the ligand exchange reaction, their relaxivities are still comparable to those of commercial nanoparticle-based MRI contrast agents (Nordmeyer et al. 2014).

Cao et al. (2016a) reported a mixed polymeric micellar MRI contrast agent with a hydrodynamic diameter of about 85 nm that exhibited much higher r1 relaxivity (14.01 mM^{-1} S^{-1}) than commercial Magnevist® (3.95 mM^{-1} S^{-1}). Although dendrimers with uniform hyperbranched structures are known as one of the best supports for imaging probe and drug delivery, their biological applications are limited due to their complicated and multi-step synthesis methods and poor biocompatibility. Han et al. (2016) reported an efficient method for the synthesis of zwitterionic polyglycerol dendrimers with a β-cyclodextrin core as MRI contrast agent carriers. Cao et al. (2016b) synthesized a linear macromolecular contrast agent with a composition of polyglycerol as a backbone and partial hydroxyl connected with gadolinium labeled poly (L-lysine) dendrons. A ring-opening polymerization reaction has been used for the synthesis of polyglycerol-coated magnetic iron oxide nanoparticles applying hexanoic acid as a linker (Fig. 17). However, Wang et al. (2009) used this method to prepare composite nanoparticles with a diameter of 23.0 ± 0.3 nm that were highly stable in both aqueous and cell culture media. Chemical stability under physiological conditions is known as one of the most important

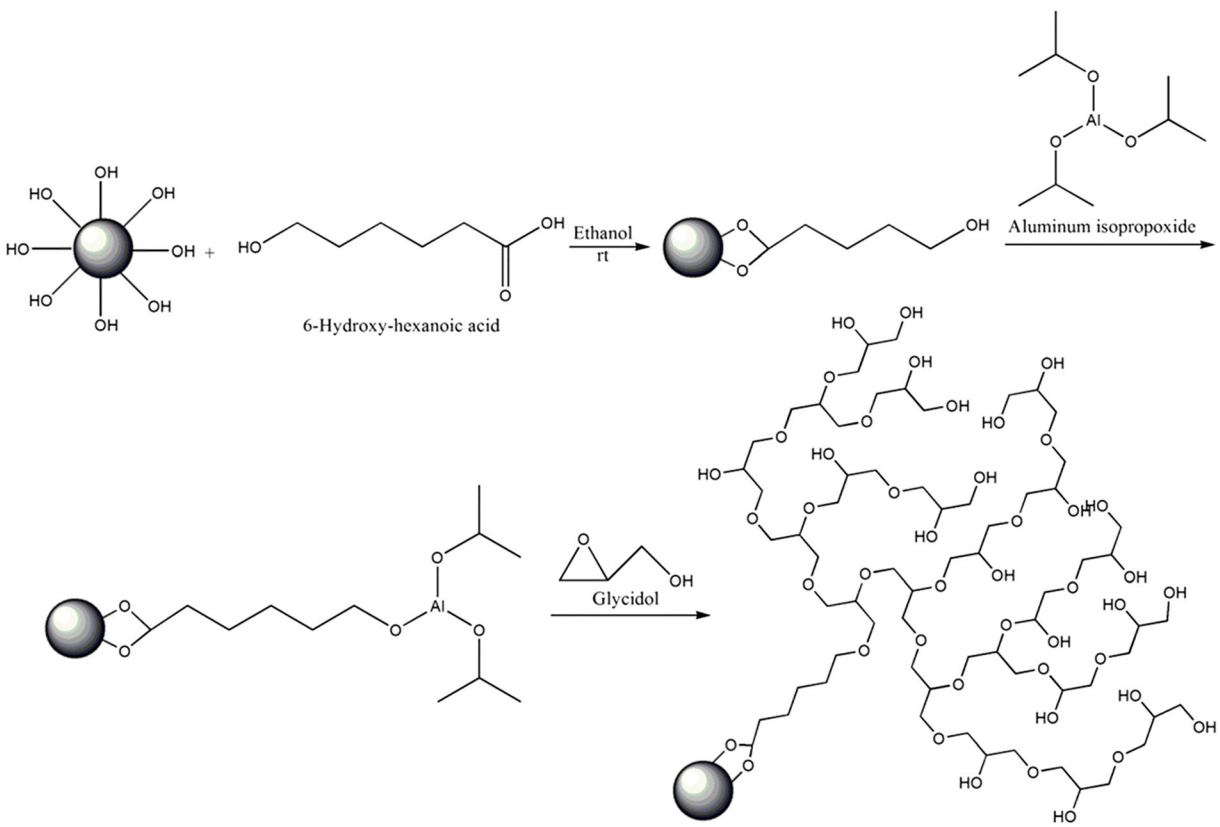

Fig. 17 Superparamagnetic hyper-branched Fe_3O_4@polyglycerol nanoparticles applied as a MRI contrast agent

properties of nanoparticles for their use as injectable MRI agents.

Miscellaneous polymers

Polymeric liposome–coated superparamagnetic iron oxide nanoparticles with a targeting ligand and the ability of transferring from organic phases to aqueous solutions have been evaluated as a magnetic resonance imaging contrast agent. The obtained results from the investigation of Liao et al. (2011) demonstrated a narrow range of size dispersity with a core size of about 8–10 nm and T2 relaxivities of 164.14 mM^{-1} s^{-1}.

Zhou et al. (2010) obtained superparamagnetic fulvic acid-coated iron oxide nanoparticles by co-precipitation of iron salts and small molecules of fulvic acid as stabilizers. Transmission electron microscopy observations showed that the prepared nanoparticles had a diameter of about 10 nm. In addition, fulvic acid–coated magnetic nanoparticles showed proper T2 relaxation rates, which make them suitable as contrast agent for MRI of liver because of their increased sensitivity leading to the differentiation between normal and pathologic tissues in the liver.

Polypyrrole coated-magnetic nanoparticles were reported by Tian et al. (2014) with an r2 value of 290.91 mM^{-1} S^{-1}, which was higher than those of some commercially available MRI contrast agents such as Feridex (152 mM^{-1} S^{-1}) and Resovist (86 mM^{-1} S^{-1}). Moreover, a hybrid composite has been reported as a contrast agent for MRI of liver tumors consisting of superparamagnetic iron oxide nanoshells and doxorubicin as an anticancer (Wang et al. 2014).

Conclusion and future prospective

In summary, this review discussed several important aspects of organic/inorganic polymer-coated iron oxide nanoparticles as MRI contrast agents that are progressively studied for the past few years. Iron oxide ultrasmall nanoparticles have been efficiently synthesized via some methods such as high-temperature co-precipitation, thermal decomposition, and polyol approaches. Although polyol methods are feasible for large-scale production of magnetic nanoparticles, thermal decomposition and co-precipitation methods are highly efficient by controlling the reaction conditions affecting the relaxation properties of the nanoparticles such as the size and surface capping molecules. The development of iron oxide nanoparticles as MRI contrast agents may lead to the focus of major research on the integration of MRI with other imaging techniques such as positron emission tomography and computed tomography. Numerous studies have shown that iron oxide contrast agents are less toxic than gadolinium-based contrast agents; however, the development of magnetic contrast agents is still in its infancy and studies on in vitro and in vivo biocompatibility, bio-distribution, pharmacokinetics, and toxicity should be considered for their further potential clinical applications. Although iron oxide particles offer many perspectives for in vitro and in vivo researches, it seems that the particles might be developed as the future MRI contrast agents for human clinical applications.

Declarations

Competing Interest The authors declare no competing interests.

References

Abbate V, Hider R (2017) Iron in biology. Metallomics 9:1467–1469. https://doi.org/10.1039/C7MT90039B

Akbar A, Riaz S, Ashraf R, Naseem S (2015) Magnetic and magnetization properties of iron oxide thin films by microwave assisted sol–gel route. J Sol-Gel Sci Technol 74:320–328. https://doi.org/10.1007/s10971-014-3528-9

Arimoto R, Balsam W, Schloesslin C (2002) Visible spectroscopy of aerosol particles collected on filters: iron-oxide minerals. Atmos Environ 36:89–96. https://doi.org/10.1016/S1352-2310(01)00465-4

Arsalani N, Fattahi H, Laurent S, Burtea C, Elst LV, Muller RN (2012) Polyglycerol-grafted superparamagnetic iron oxide nanoparticles: highly efficient MRI contrast agent for liver and kidney imaging and potential scaffold for cellular and molecular imaging. Contrast Media Mol Imaging 7:185–194. https://doi.org/10.1002/cmmi.479

Bar-Shir A, Avram L, Yariv-Shoushan S, Anaby D, Cohen S, Segev-Amzaleg N, Frenkel D, Sadan O, Offen D, Cohen Y (2014) Alginate-coated magnetic nanoparticles for noninvasive MRI of extracellular calcium. NMR Biomed 27:774–783. https://doi.org/10.1002/nbm.3117

Basly B, Felder-Flesch D, Perriat P, Billotey C, Taleb J, Pourroy G, Begin-Colin S (2010) Dendronized iron oxide nanoparticles as contrast agents for MRI. Chem Commun 46:985–987. https://doi.org/10.1039/B920348F

Basly B, Popa G, Fleutot S, Pichon BP, Garofalo A, Ghobril C, Billotey C, Berniard A, Bonazza P, Martinez H, Felder-Flesch D, Begin-Colin S (2013) Effect of the nanoparticle synthesis method on dendronized iron oxides as MRI

contrast agents. Dalton Trans 42:2146–2157. https://doi.org/10.1039/C2DT31788E

Bautista MC, Bomati-Miguel O, Zhao X, Morales MP, Gonzalez-Carreno T, Pérez de Alejo R, Ruiz-Cabello J, Veintemillas-Verdaguer S (2004) Comparative study of ferrofluids based on dextran-coated iron oxide and metal nanoparticles for contrast agents in magnetic resonance imaging. Nanotechnology 15:154–159. https://doi.org/10.1088/0957-4484/15/4/008

Bautista MC, Bomati-Miguel O, del Puerto MM, Serna CJ, Veintemillas-Verdaguer S (2005) Surface characterisation of dextran-coated iron oxide nanoparticles prepared by laser pyrolysis and coprecipitation. J Magn Magn Mater 293:20–27. https://doi.org/10.1016/j.jmmm.2005.01.038

Beg MS, Mohapatra J, Pradhan L, Patkar D, Bahadur D (2017) Porous Fe_3O_4-SiO_2 core-shell nanorods as high-performance MRI contrast agent and drug delivery vehicle. J Magn Magn Mater 428:340–347. https://doi.org/10.1016/j.jmmm.2016.12.079

Behzadi AH, Zhao Y, Farooq Z, Prince MR (2017) Immediate allergic reactions to gadolinium-based contrast agents: a systematic review and meta-analysis. Radiology 286:471–482. https://doi.org/10.1148/radiol.2017162740

Berger F, Kubik-Huch RA, Niemann T, Schmid HR, Poetzsch M, Froehlich JM, Beer JH, Kraemer T (2018) Gadolinium distribution in cerebrospinal fluid after administration of a gadolinium-based MR contrast agent in humans. Radiology 288:703–709. https://doi.org/10.1148/radiol.2018171829

Blahut J, Bernášek K, Gálisová A, Herynek V, Císařová I, Kotek J, Lang J, Matějková S, Hermann P (2017) Paramagnetic ^{19}F relaxation enhancement in nickel (II) complexes of N-trifluoroethyl cyclam derivatives and cell labeling for ^{19}F MRI. Inorg Chem 56:13337–11348. https://doi.org/10.1021/acs.inorgchem.7b02119

Blumfield E, Moore MM, Drake MK, Goodman TR, Lewis KN, Meyer LT, Ngo TD, Sammet C, Stanescu AL, Swenson DW, Slovis TL, Iyer RS (2017) Survey of gadolinium-based contrast agent utilization among the members of the Society for Pediatric Radiology: a Quality and Safety Committee report. Pediatr Radiol 47:665–673. https://doi.org/10.1007/s00247-017-3807-z

Bonnet CS, Fries PH, Crouzy S, Delangle P (2010) Outer-sphere investigation of MRI relaxation contrast agents. Example of a cyclodecapeptide gadolinium complex with second-sphere water. J Phys Chem 114:8770–8781. https://doi.org/10.1021/jp101443v

Boyer C, Whittaker MR, Bulmus V, Liu J, Davis TP (2010) The design and utility of polymer-stabilized iron-oxide nanoparticles for nanomedicine applications. NPG Asia Mater 2:23–30. https://doi.org/10.1038/asiamat.2010.6

Bulte JW, de Jonge MW, Kamman RL, Go KG, Zuiderveen F, Blaauw B, Oosterbaan JA, Hauw T, de Leij L (1992) Dextran-magnetite particles: contrast-enhanced MRI of blood–brain barrier disruption in a rat model. Magn Reson Med 23:215–223. https://doi.org/10.1002/mrm.1910230203

Bulte JWM, Douglas T, Witwer B, Zhang S-C, Strable E, Lewis BK, Zywicke H, Miller B, van Gelderen P, Moskowitz BM, Duncan ID, Frank JA (2001) Magnetodendrimers allow endosomal magnetic labeling and in vivo tracking of stem cells. Nat Biotechnol 19:1141–1147. https://doi.org/10.1038/nbt1201-1141

Cai H, Li K, Li J, Wen S, Chen Q, Shen M, Zheng L, Zhang G, Shi X (2015) Dendrimer-assisted formation of Fe_3O_4/Au nanocomposite particles for targeted dual mode CT/MR imaging of tumors. Small 11:4584–4593. https://doi.org/10.1002/smll.201500856

Cao Y, Liu M, Zhang K, Zu G, Kuang Y, Tong X, Xiong D, Pei R (2016a) Poly (glycerol) used for constructing mixed polymeric micelles as T1 MRI contrast agent for tumor-targeted imaging. Biomacromolecules 18:150–158. https://doi.org/10.1021/acs.biomac.6b01437

Cao Y, Liu M, Zhang K, Dong J, Zu G, Chen Y, Zhang T, Xiong D, Pei R (2016b) Preparation of linear poly (glycerol) as a T 1 contrast agent for tumor-targeted magnetic resonance imaging. J Mater Chem 4:6716–6725. https://doi.org/10.1039/C6TB01514J

Caravan P (2006) Strategies for increasing the sensitivity of gadolinium based MRI contrast agents. Chem Soc Rev 35:512–523. https://doi.org/10.1039/B510982P

Chang Y, Liu N, Chen L, Meng X, Liu Y, Li Y, Wang J (2012a) Synthesis and characterization of DOX-conjugated dendrimer-modified magnetic iron oxide conjugates for magnetic resonance imaging, targeting, and drug delivery. J Mater Chem 22:9594–9601. https://doi.org/10.1039/C2JM16792A

Chang Y, Liu N, Chen L, Meng X, Liu Y, Li Y, Wang J (2012b) Synthesis and characterization of DOX-conjugated dendrimer-modified magnetic iron oxide conjugates for magnetic resonance imaging, targeting, and drug delivery. J. Mater. Chem. 22:9594–9601. https://doi.org/10.1039/C2JM16792A

Chen TJ, Cheng TH, Chen CY, Hsu SC, Cheng TL, Liu GC, Wang YM (2009) Targeted Herceptin–dextran iron oxide nanoparticles for noninvasive imaging of HER2/neu receptors using MRI. J Biol Inorg Chem 14:253–260. https://doi.org/10.1007/s00775-008-0445-9

Chen YJ, Tao J, Xiong F, Zhu JB, Gu N, Geng KK (2010) Characterization and in vitro cellular uptake of PEG coated iron oxide nanoparticles as MRI contrast agent. Pharmazie 65:481–486

Chen W, Lu F, Chen CCV, Mo KC, Hung Y, Guo ZX, Lin C-H, Lin M-H, Lin Y-H, Chang C, Mou C-Y (2013) Manganese-enhanced MRI of rat brain based on slow cerebral delivery of manganese (II) with silica-encapsulated $MnxFe_{1-x}O$ nanoparticles. NMR Biomed 26:1176–1185. https://doi.org/10.1002/nbm.2932

Cheng C, Xu F, Gu H (2011) Facile synthesis and morphology evolution of magnetic iron oxide nanoparticles in different polyol processes. New J Chem 35:1072–1079. https://doi.org/10.1039/C0NJ00986E

Cheng Z, Dai Y, Kang X, Li C, Huang S, Lian H, Hou Z, Ma P, Lin J (2014) Gelatin-encapsulated iron oxide nanoparticles for platinum (IV) prodrug delivery, enzyme-stimulated release and MRI. Biomaterials 35:6359–6368. https://doi.org/10.1016/j.biomaterials.2014.04.029

Cheng W, Xu X, Wu F, Li J (2016) Synthesis of cavity-containing iron oxide nanoparticles by hydrothermal treatment of colloidal dispersion. Mater Lett 164:210–212. https://doi.org/10.1016/j.matlet.2015.10.170

Clauson RM, Chen M, Scheetz LM, Berg B, Chertok B (2018) Size-controlled iron oxide nanoplatforms with lipidoid-stabilized shells for efficient magnetic resonance imaging-trackable lymph node targeting and high-capacity

biomolecule display. ACS Appl Mater Interfaces 8:20281–20295. https://doi.org/10.1021/acsami.8b02830

Coe CL, Lubach GR, Kling P, Georgieff M, Rao R, Connor J (2015) Iron biology is key to understanding how inflammation, stress and obesity affect maternal and child health, Brain, Behavior, and. Immunity. 49:e34. https://doi.org/10.1016/j.bbi.2015.06.132

Cui X, Antonietti M, Yu SH (2006) Structural effects of iron oxide nanoparticles and iron ions on the hydrothermal carbonization of starch and rice carbohydrates. Small 2:756–759. https://doi.org/10.1002/smll.200600047

Dadfar SM, Roemhild K, Drude NI, von Stillfried S, Knüchel R, Kiessling F, Lammers T (2019) Iron oxide nanoparticles: diagnostic, therapeutic and theranostic applications. Adv Drug Delivery Rev 138:302–325. https://doi.org/10.1016/j.addr.2019.01.005

Dai F, Du M, Liu Y, Liu G, Liu Q, Zhang X (2014a) Folic acid-conjugated glucose and dextran coated iron oxide nanoparticles as MRI contrast agents for diagnosis and treatment response of rheumatoid arthritis. J Mater Chem 2:2240–2247. https://doi.org/10.1039/C3TB21732A

Dai L, Liu Y, Wang Z, Guo F, Shi D, Zhang B (2014b) One-pot facile synthesis of PEGylated superparamagnetic iron oxide nanoparticles for MRI contrast enhancement. Mater Sci Eng 41:161–167. https://doi.org/10.1016/j.msec.2014.04.041

Darbandi M, Laurent S, Busch M, Li Z-A, Yuan Y, Krüger M, Farle M, Winterer M, Elst LV, Muller RN, Wende H (2013) Blocked-micropores, surface functionalized, bio-compatible and silica-coated iron oxide nanocomposites as advanced MRI contrast agent. J Nanopart Res 15:1664–1669. https://doi.org/10.1007/s11051-013-1664-8

Dekkers IA, Roos R, van der Molen AJ (2018) Gadolinium retention after administration of contrast agents based on linear chelators and the recommendations of the European Medicines Agency. Eur Radiol 28:1579–1584. https://doi.org/10.1007/s00330-017-5065-8

El-Boubbou K (2018) Magnetic iron oxide nanoparticles as drug carriers: preparation, conjugation and delivery. Nanomedicine 13:929–952. https://doi.org/10.2217/nnm-2017-0320

Fakayode OJ, Songca SP, Oluwafemi OS (2018) Neutral red separation property of ultrasmall-gluconic acid capped superparamagnetic iron oxide nanoclusters coprecipitated with goethite and hematite. Sep Purif Technol 192:475–482. https://doi.org/10.1016/j.seppur.2017.09.050

Fraum TJ, Ludwig DR, Bashir MR, Fowler KJ (2017) Gadolinium-based contrast agents: a comprehensive risk assessment. J Magn Reson Imaging 46:338–353. https://doi.org/10.1002/jmri.25625

Gao GH, Lee JW, Nguyen MK, Im GH, Yang J, Heo H, Jeon P, Park TG, Lee JH, Lee DS (2011) pH-responsive polymeric micelle based on PEG-poly (β-amino ester)/(amido amine) as intelligent vehicle for magnetic resonance imaging in detection of cerebral ischemic area. J Controlled Release 155:11–17. https://doi.org/10.1016/j.jconrel.2010.09.012

Gash AE, Tillotson TM, Satcher JH, Poco JF, Hrubesh LW, Simpson RL (2001) Use of epoxides in the sol−gel synthesis of porous iron (III) oxide monoliths from Fe (III) salts. Chem Mater 13:999–1007. https://doi.org/10.1021/cm0007611

Ge S, Shi X, Sun K, Li C, Uher C, Baker JR, Horr MMB, Orr BG (2009) Facile hydrothermal synthesis of iron oxide nanoparticles with tunable magnetic properties. J Phys Chem C 113:13593–13599. https://doi.org/10.1021/jp902953t

Gómez-Vallejo V, Puigivila M, Plaza-García S, Szczupak B, Piñol R, Murillo JL, Sorribas V, Lou G, Veintemillas S, Ramos-Cabrer P, Llop J, Millán A (2018) PEG-copolymer-coated iron oxide nanoparticles that avoid the reticuloendothelial system and act as kidney MRI contrast agents. Nanoscale 10:14153–14164. https://doi.org/10.1039/C8NR03084G

Grover VP, Tognarelli JM, Crossey MM, Cox IJ, Taylor-Robinson SD, McPhail MJ (2015) Magnetic resonance imaging: principles and techniques: lessons for clinicians. J Clin Exp Hepatol 5:246–255. https://doi.org/10.1016/j.jceh.2015.08.001

Gyergyek S, Makovec D, Jagodič M, Drofenik M, Schenk K, Jordan O, Kovač J, Dražič G, Hofmann H (2017) Hydrothermal growth of iron oxide NPs with a uniform size distribution for magnetically induced hyperthermia: structural, colloidal and magnetic properties. J Alloys Compd 694:261–271. https://doi.org/10.1016/j.jallcom.2016.09.238

Hachani R, Lowdell M, Birchall M, Hervault A, Mertz D, Begin-Colin S, Thanh NTK (2016) Polyol synthesis, functionalisation, and biocompatibility studies of superparamagnetic iron oxide nanoparticles as potential MRI contrast agents. Nanoscale 8:3278–3287. https://doi.org/10.1039/C5NR03867G

Hajela S, Botta M, Giraudo S, Xu J, Raymond KN, Aime S (2000) A tris-hydroxymethyl-substituted derivative of Gd-TREN-Me-3, 2-HOPO: an MRI relaxation agent with improved efficiency. J Am Chem Soc 122:11228–11129. https://doi.org/10.1021/ja994315u

Han Y, Qian Y, Zhou X, Hu H, Liu X, Zhou Z, Tang J, Shen Y (2016) Facile synthesis of zwitterionic polyglycerol dendrimers with a β-cyclodextrin core as MRI contrast agent carriers. Polym Chem 7:6354–6362. https://doi.org/10.1039/C6PY01404F

Hao R, Xing R, Xu Z, Hou Y, Gao S, Sun S (2010) Synthesis, functionalization, and biomedical applications of multifunctional magnetic nanoparticles. Adv Mater 22:2729–2742. https://doi.org/10.1002/adma.201000260

Haw CY, Mohamed F, Chia CH, Radiman S, Zakaria S, Huang NM, Lim HN (2010) Hydrothermal synthesis of magnetite nanoparticles as MRI contrast agents. Ceram Int 36:1417–1422. https://doi.org/10.1016/j.ceramint.2010.02.005

Hedayati M, Abubaker-Sharif B, Khattab M, Razavi A, Mohammed I, Nejad A, Wabler M, Zhou H, Mihalic J, Gruettner C, de Weese T (2018) An optimised spectrophotometric assay for convenient and accurate quantitation of intracellular iron from iron oxide nanoparticles. Int J Hyperth 34:373–381. https://doi.org/10.1080/02656736.2017.1354403

Henkelman RM, Stanisz GJ, Graham SJ (2001) Magnetization transfer in MRI: a review. NMR Biomed 14:57–64. https://doi.org/10.1002/nbm.683

Hermann P, Kotek J, Kubíček V, Lukeš I (2008) Gadolinium (III) complexes as MRI contrast agents: ligand design and properties of the complexes. Dalton Trans 23:3027–3047. https://doi.org/10.1039/B719704G

Hillman AL, Schwartz JS (1985) The adoption and diffusion of CT and MRI in the United States: a comparative analysis.

Med Care 1:1283–1294 https://www.jstor.org/stable/3765051

Hong RY, Feng B, Chen LL, Liu GH, Li HZ, Zheng Y, Wei DG (2008) Synthesis, characterization and MRI application of dextran-coated Fe_3O_4 magnetic nanoparticles. Biochem Eng J 42:290–300. https://doi.org/10.1016/j.bej.2008.07.009

Hu F, Jia Q, Li Y, Gao M (2011) Facile synthesis of ultrasmall PEGylated iron oxide nanoparticles for dual-contrast T1-and T2-weighted magnetic resonance imaging. Nanotechnology 22:245604. https://doi.org/10.1088/0957-4484/22/24/245604

Huang J, Bu L, Xie J, Chen K, Cheng Z, Li X, Chen X (2010) Effects of nanoparticle size on cellular uptake and liver MRI with polyvinylpyrrolidone-coated iron oxide nanoparticles. ACS Nano 4:7151–7160. https://doi.org/10.1021/nn101643u

Hurley KR, Ring HL, Etheridge M, Zhang J, Gao Z, Shao Q, Klein ND, Szlag VM, Chung C, Reineke TM, Garwood M, Bischof JC, Haynes C (2016) Predictable heating and positive MRI contrast from a mesoporous silica-coated iron oxide nanoparticle. Mol Pharmaceutics 13:2172–2183. https://doi.org/10.1021/acs.molpharmaceut.5b00866

Hussain NHI, Mustafa MK, Asman S (2018) Synthesis of PANI/iron (II, III) oxide hybrid nanocomposites using sol-gel method. J Sci Technol 10:1–4 https://doi.org/10.0.120.160/jst.2018.10.01.001

Iqbal MZ, Ma X, Chen T, Zhang LE, Ren W, Xiang L, Wu A (2015) Silica-coated super-paramagnetic iron oxide nanoparticles (SPIONPs): a new type contrast agent of T1 magnetic resonance imaging (MRI). J Mater Chem B 3:5172–5181. https://doi.org/10.1039/C5TB00300H

Jang H, Lee C, Nam GE, Quan B, Choi HJ, Yoo JS, Piao Y (2016) In vivo magnetic resonance and fluorescence dual imaging of tumor sites by using dye-doped silica-coated iron oxide nanoparticles. J Nanopart Res 18:41–45. https://doi.org/10.1007/s11051-016-3353-x

Juang JH, Wang JJ, Shen CR, Kuo CH, Chien YW, Kuo HY, Chien Y-W, Kuo H-Y, Tsai Z-T, Yen T-C (2010) Magnetic resonance imaging of transplanted mouse islets labeled with chitosan-coated superparamagnetic iron oxide nanoparticles. Transplant Proc 42:2104–2108. https://doi.org/10.1016/j.transproceed.2010.05.103

Kandasamy G, Maity D (2015) Recent advances in superparamagnetic iron oxide nanoparticles (SPIONs) for in vitro and in vivo cancer nanotheranostics. Int J Pharmaceutics 496:191–218. https://doi.org/10.1016/j.ijpharm.2015.10.058

Kaur G, Dogra V, Kumar R, Kumar S, Singh K (2018) Fabrication of iron oxide nanocolloids using metallosurfactant-based microemulsions: antioxidant activity, cellular, and genotoxicity toward *Vitis vinifera*. J Biomol Struct Dyn 37:892–909. https://doi.org/10.1080/07391102.2018.1442251

Kielar F, Cassino C, Leone L, Tei L, Botta M (2018) Macrocyclic trinuclear gadolinium (iii) complexes: the influence of the linker flexibility on the relaxometric properties. New J Chem 42:7984–7992. https://doi.org/10.1039/C7NJ04696K

Kim DK, Zhang Y, Voit W, Rao KV, Muhammed M (2001) Synthesis and characterization of surfactant-coated superparamagnetic monodispersed iron oxide nanoparticles. J Magn Magn Mater 225:30–36. https://doi.org/10.1016/S0304-8853(00)01224-5

Kim EH, Ahn Y, Lee HS (2007) Biomedical applications of superparamagnetic iron oxide nanoparticles encapsulated within chitosan. J Alloys Compd 434:633–636. https://doi.org/10.1016/j.jallcom.2006.08.311

Kumagai M, Imai Y, Nakamura T, Yamasaki Y, Sekino M, Ueno S, Hanaoka K, Kikuchi K, Nagano T, Kaneko E, Shimokado K, Kataoka K (2007) Iron hydroxide nanoparticles coated with poly (ethylene glycol)-poly (aspartic acid) block copolymer as novel magnetic resonance contrast agents for in vivo cancer imaging. Colloids Surf B 56:174–181. https://doi.org/10.1016/j.colsurfb.2006.12.019

Lamanna G, Kueny-Stotz M, Mamlouk-Chaouachi H, Ghobril C, Basly B, Bertin A, Miladi I, Billotey C, Pourroy G, Begin-Colin S, Felder-Flesch D (2011) Dendronized iron oxide nanoparticles for multimodal imaging. Biomaterials 32:8562–8573. https://doi.org/10.1016/j.biomaterials.2011.07.026

Lassoued A, Dkhil B, Gadri A, Ammar S (2017) Control of the shape and size of iron oxide (α-Fe_2O_3) nanoparticles synthesized through the chemical precipitation method. Results phys 7:3007–3015. https://doi.org/10.1016/j.rinp.2017.07.066

Lassoued A, Lassoued MS, Dkhil B, Ammar S, Gadri A (2018) Synthesis, photoluminescence and magnetic properties of iron oxide (α-Fe_2O_3) nanoparticles through precipitation or hydrothermal methods. Phys E 101:212–219. https://doi.org/10.1016/j.physe.2018.04.009

Laurent S, Forge D, Port M, Roch A, Robic C, Vander Elst L, Muller RN (2008) Magnetic iron oxide nanoparticles: synthesis, stabilization, vectorization, physicochemical characterizations, and biological applications. Chem Rev 108:2064–2110. https://doi.org/10.1021/cr068445e

Lee N, Hyeon T (2012) Designed synthesis of uniformly sized iron oxide nanoparticles for efficient magnetic resonance imaging contrast agents. Chem Soc Rev 41:2575–2589. https://doi.org/10.1039/C1CS15248C

Lee H, Shao H, Huang Y, Kwak B (2005) Synthesis of MRI contrast agent by coating superparamagnetic iron oxide with chitosan. IEEE Trans Magn 41:4102–4104. https://doi.org/10.1109/TMAG.2005.855338

Lee HY, Lee SH, Xu C, Xie J, Lee JH, Wu B, Koh AL, Wang X, Sinclair R, Wang SX, Nishimura DG, Biswal S, Sun S, Cho SH, Chen X (2008) Synthesis and characterization of PVP-coated large core iron oxide nanoparticles as an MRI contrast agent. Nanotechnology 19:165101. https://doi.org/10.1088/0957-4484/19/16/165101

Li J, Shi X, Shen M (2014) Hydrothermal synthesis and functionalization of iron oxide nanoparticles for MR imaging applications. Part Part Syst Charact 31:1223–1237. https://doi.org/10.1002/ppsc.201400087

Li D, Li SJ, Zhang Y, Jiang JJ, Gong WJ, Wang JH, Zhang ZD (2015) Monodisperse water-soluble-Fe_2O_3/polyvinylpyrrolidone nanoparticles for a magnetic resonance imaging contrast agent. Mater Res Innov 19:58–62. https://doi.org/10.1179/1432891715Z.0000000001428

Liao Z, Wang H, Lv R, Zhao P, Sun X, Wang S, Su W, Niu R, Chang J (2011) Polymeric liposomes-coated superparamagnetic iron oxide nanoparticles as contrast agent for targeted magnetic resonance imaging of cancer cells. Langmuir 27:3100–3105. https://doi.org/10.1021/la1050157

Lin S, Lin K, Lu D, Liu Z (2017) Preparation of uniform magnetic iron oxide nanoparticles by co-precipitation in a helical module microchannel reactor. J Environ Chem Eng 5:303–309. https://doi.org/10.1016/j.jece.2016.12.011

Liu G, Sobering G, Duyn J, Moonen CT (1993) A functional MRI technique combining principles of echo-shifting with a train of observations (PRESTO). Magn Reson Med 30:764–768. https://doi.org/10.1002/mrm.1910300617

Liu DF, Qian C, An YL, Chang D, Ju SH, Teng GJ (2014) Magnetic resonance imaging of post-ischemic blood–brain barrier damage with PEGylated iron oxide nanoparticles. Nanoscale 6:15161–15167. https://doi.org/10.1039/C4NR03942D

Liu J, Xu J, Zhou J, Zhang Y, Guo D, Wang Z (2017) Fe_3O_4-based PLGA nanoparticles as MR contrast agents for the detection of thrombosis. Int J Nanomed 12:1113–1126. https://doi.org/10.2147/IJN.S123228

Lohrke J, Frenzel T, Endrikat J, Alves FC, Grist TM, Law M, Lee JM, Leiner T, Li K-C, Nikolaou K, Prince MR, Schild HH, Weinreb JC, Yoshikawa K, Pietsch H (2016) 25 years of contrast-enhanced MRI: developments, current challenges and future perspectives. Adv Ther 33:1–28. https://doi.org/10.1007/s12325-015-0275-4

López-Ramón MV, Álvarez MA, Moreno-Castilla C, Fontecha-Cámara MA, Yebra-Rodríguez Á, Bailón-García E (2018) Effect of calcination temperature of a copper ferrite synthesized by a sol-gel method on its structural characteristics and performance as Fenton catalyst to remove gallic acid from water. J Colloid Interface Sci 511:193–202. https://doi.org/10.1016/j.jcis.2017.09.117

Lu Y, Yin Y, Mayers BT, Xia Y (2002) Modifying the surface properties of superparamagnetic iron oxide nanoparticles through a sol−gel approach. Nano Lett 2:183–186. https://doi.org/10.1021/nl015681q

Lunvongsa S, Oshima M, Motomizu S (2006) Determination of total and dissolved amount of iron in water samples using catalytic spectrophotometric flow injection analysis. Talanta 68:969–973. https://doi.org/10.1016/j.talanta.2005.06.067

Luong D, Sau S, Kesharwani P, Iyer AK (2017) Polyvalent folate-dendrimer-coated iron oxide theranostic nanoparticles for simultaneous magnetic resonance imaging and precise cancer cell targeting. Biomacromolecules 18:1197–1209. https://doi.org/10.1021/acs.biomac.6b01885

Lutz JF, Stiller S, Hoth A, Kaufner L, Pison U, Cartier R (2006) One-pot synthesis of PEGylated ultrasmall iron-oxide nanoparticles and their in vivo evaluation as magnetic resonance imaging contrast agents. Biomacromolecules 7:3132–3138. https://doi.org/10.1021/bm0607527

Ma HL, Qi XR, Maitani Y, Nagai T (2007) Preparation and characterization of superparamagnetic iron oxide nanoparticles stabilized by alginate. Int J Pharm 333:177–186. https://doi.org/10.1021/bm0607527

Ma HL, Xu YF, Qi XR, Maitani Y, Nagai T (2008) Superparamagnetic iron oxide nanoparticles stabilized by alginate: pharmacokinetics, tissue distribution, and applications in detecting liver cancers. Int J Pharm 354:217–226. https://doi.org/10.1016/j.ijpharm.2007.11.036

Maghsodi A, Adlnasab L, Shabanian M, Javanbakht M (2018) Optimization of effective parameters in the synthesis of nanopore anodic aluminum oxide membrane and arsenic removal by prepared magnetic iron oxide nanoparicles in anodic aluminum oxide membrane via ultrasonic-hydrothermal method. Ultrason Sonochem 48:441–452. https://doi.org/10.1016/j.ultsonch.2018.07.003

Mahmed N, Heczko O, Lancok A, Hannula SP (2014) The magnetic and oxidation behavior of bare and silica-coated iron oxide nanoparticles synthesized by reverse co-precipitation of ferrous ion (Fe^{2+}) in ambient atmosphere. J Magn Magn Mater 353:15–22. https://doi.org/10.1016/j.jmmm.2013.10.012

Mallakpour S, Madani M (2015) A review of current coupling agents for modification of metal oxide nanoparticles. Prog Org Coat 86:194–207. https://doi.org/10.1016/j.porgcoat.2015.05.023

Mansfield P, Glover P, Bowtell R (1994) Active acoustic screening: design principles for quiet gradient coils in MRI. Meas Sci Technol 5:1021. https://doi.org/10.1088/0957-0233/5/8/026

Masoudi A, Hosseini HRM, Shokrgozar MA, Ahmadi R, Oghabian MA (2012) The effect of poly (ethylene glycol) coating on colloidal stability of superparamagnetic iron oxide nanoparticles as potential MRI contrast agent. Int J Pharm 433:129–141. https://doi.org/10.1016/j.ijpharm.2012.04.080

Mogharabi-Manzari M, Amini M, Abdollahi M, Khoobi M, Bagherzadeh G, Faramarzi MA (2018a) Co-immobilization of Laccase and TEMPO in the Compartments of Mesoporous Silica for a Green and One-Pot Cascade Synthesis of Coumarins by Knoevenagel Condensation. ChemCatChem 10:1542–1546. https://doi.org/10.1002/cctc.201701527

Mogharabi-Manzari M, Kiani M, Aryanejad S, Imanparast S, Amini M, Faramarzi MA (2018b) A magnetic heterogeneous biocatalyst composed of immobilized laccase and 2,2,6,6-tetramethylpiperidine-1-oxyl (TEMPO) for green one-pot cascade synthesis of 2-substituted benzimidazole and benzoxazole derivatives under mild reaction conditions. Adv Syn Catal 360:3563–3571. https://doi.org/10.1002/adsc.201800459

Mogharabi-Manzari M, Ghahremani MH, Sedaghat T, Shayan F, Faramarzi MA (2019a) A laccase heterogeneous magnetic fibrous silica-based biocatalyst for green and one-pot cascade synthesis of chromene derivatives. Eur J Org Chem 2019:1741–1747. https://doi.org/10.1002/ejoc.201801784

Mogharabi-Manzari M, Heydari M, Sadeghian-Abadi S, Yousefi-Mokri M, Faramarzi MA (2019b) Enzymatic dimerization of phenylacetylene by laccase immobilized on magnetic nanoparticles via click chemistry. Biocatal Biotransform 37:455–465. https://doi.org/10.1080/10242422.2019.1611788

Morales MP, Bomati-Miguel O, de Alejo RP, Ruiz-Cabello J, Veintemillas-Verdaguer S, O'Grady K (2003) Contrast agents for MRI based on iron oxide nanoparticles prepared by laser pyrolysis. J Magn Magn Mater 266:102–109. https://doi.org/10.1016/S0304-8853(03)00461-X

Moser FG, Watterson CT, Weiss S, Austin M, Mirocha J, Prasad R, Wang J (2018) High signal intensity in the dentate nucleus and globus pallidus on unenhanced T1-weighted MR images: comparison between gadobutrol and linear gadolinium-based contrast agents. Am J Neuroradiol 39:421–426. https://doi.org/10.3174/ajnr.A5538

Mukh-Qasem RA, Gedanken A (2005) Sonochemical synthesis of stable hydrosol of Fe_3O_4 nanoparticles. J Colloid Interface Sci 284:489–494. https://doi.org/10.1016/j.jcis.2004.10.073

Nadeem M, Ahmad M, Akhtar MS, Shaari A, Riaz S, Naseem S, Masood M, Saeed MA (2016) Magnetic properties of polyvinyl alcohol and doxorubicine loaded iron oxide nanoparticles for anticancer drug delivery applications. Plos One 11: e0158084. https://doi.org/10.1371/journal.pone.0158084

Naha PC, Zaki AA, Hecht E, Chorny M, Chhour P, Blankemeyer E, Yates DM, Witschey WRT, Litt HI, Tsourkas A, Cormode DP (2014) Dextran coated bismuth–iron oxide nanohybrid contrast agents for computed tomography and magnetic resonance imaging. J Mater Chem B 2:8239–8248. https://doi.org/10.1039/C4TB01159G

Najafian N, Shanehsazzadeh S, Hajesmaeelzadeh F, Lahooti A, Gruettner C, Oghabian MA (2015) Effect of functional group and surface charge of PEGand dextran-coated USPIO as a contrast agentin MRI on relaxivity constant. Appl Magn Reson 46:685–692. https://doi.org/10.1007/s00723-015-0667-2

Nan A, Suciu M, Ardelean I, Şenilă M, Turcu R (2020) Characterization of the nuclear magnetic resonance relaxivity of gadolinium functionalized magnetic nanoparticles. Anal Lett. https://doi.org/10.1080/00032719.2020.1731522

Naseroleslami M, Parivar K, Khoei S, Aboutaleb N (2016) Magnetic resonance imaging of human-derived amniotic membrane stem cells using PEGylated superparamagnetic iron oxide nanoparticles. Cell J 18:332–339. https://doi.org/10.22074/cellj.2016.4560

Nielles-Vallespin S, Weber MA, Bock M, Bongers A, Speier P, Combs SE, Wöhrle J, Lehmann-Horn F, Essig M, Schad LR (2007) 3D radial projection technique with ultrashort echo times for sodium MRI: clinical applications in human brain and skeletal muscle. Magn Reson Med 57:74–81. https://doi.org/10.1002/mrm.21104

Nkansah MK, Thakral D, Shapiro EM (2011) Magnetic poly(lactide-co-glycolide) and cellulose particles for MRI-based cell tracking. Magn Reson Med 65:1776–1785. https://doi.org/10.1002/mrm.22765

Nordmeyer D, Stumpf P, Gröger D, Hofmann A, Enders S, Riese SB, Dernedde J, Taupitz M, Rauch U, Haag R, Rühl E, Graf C (2014) Iron oxide nanoparticles stabilized with dendritic polyglycerols as selective MRI contrast agents. Nanoscale 6: 9646–9654. https://doi.org/10.1039/C3NR04793H

Ozel F, Kockar H, Karaagac O (2015) Growth of iron oxide nanoparticles by hydrothermal process: effect of reaction parameters on the nanoparticle size. J Supercond Novel Magn 28:823–829. https://doi.org/10.1007/s10948-014-2707-9

Park J, Lee E, Hwang NM, Kang M, Kim SC, Hwang Y, Park J-G, Noh H-J, Kim J-Y, Park J-H, Hyeon T (2005) One-nanometer-scale size-controlled synthesis of monodisperse magnetic Iron oxide nanoparticles. Angew Chem 117: 2932–2937. https://doi.org/10.1002/anie.200461665

Park JH, von Maltzahn G, Zhang L, Schwartz MP, Ruoslahti E, Bhatia SN, Sailor MJ (2008) Magnetic iron oxide nanoworms for tumor targeting and imaging. Adv Mater 20:1630–1635. https://doi.org/10.1002/adma.200800004

Patel D, Kell A, Simard B, Deng J, Xiang B, Lin HY, Gruwel M, Tian G (2010) Cu^{2+}-labeled, SPION loaded porous silica nanoparticles for cell labeling and multifunctional imaging probes. Biomaterials 31:2866–2873. https://doi.org/10.1016/j.biomaterials.2009.12.025

Pinkas J, Reichlova V, Zboril R, Moravec Z, Bezdicka P, Matejkova J (2008) Sonochemical synthesis of amorphous nanoscopic iron(III) oxide from $Fe(acac)_3$. Ultrason Sonochem 15:257–264. https://doi.org/10.1016/j.ultsonch.2007.03.009

Plachtova P, Medříková Z, Zbořil R, Tuček J, Varma RS, Maršálek B (2018) Iron and iron oxide nanoparticles synthesized using green tea extract: differences in ecotoxicological profile and ability to degrade malachite green. ACS Sustain Chem Eng 6–7:8679–8687. https://doi.org/10.1021/acssuschemeng.8b00986

Plewes DB, Kucharczyk W (2012) Physics of MRI: a primer. J Magn Reson Imaging 35:1038–1054. https://doi.org/10.1002/jmri.23642

Pöselt E, Kloust H, Tromsdorf U, Janschel M, Hahn C, Maßlo C, Weller H (2012a) Relaxivity optimization of a PEGylated iron-oxide-based negative magnetic resonance contrast agent for T2-weighted spin-echo imaging. ACS Nano 6:1619–1624. https://doi.org/10.1021/nn204591r

Pöselt E, Kloust H, Tromsdorf U, Janschel M, Hahn C, Maßlo C, Weller H (2012b) Relaxivity optimization of a PEGylated iron-oxide-based negative magnetic resonance contrast agent for T 2-weighted spin–echo imaging. Acs Nano 6:1619–1624. https://doi.org/10.1021/nn204591r

Prince MR, Weinreb JC (2018) Notice of withdrawal: MR imaging and gadolinium: reassessing the risk of nephrogenic systemic fibrosis in patients with severe renal disease. Radiology 286:172255. https://doi.org/10.1148/radiol.2017172255

Qiao Z, Shi X (2015) Dendrimer-based molecular imaging contrast agents. Prog Polym Sci 44:1–27. https://doi.org/10.1016/j.progpolymsci.2014.08.002

Qiao R, Yang C, Gao M (2009) Superparamagnetic iron oxide nanoparticles: from preparations to in vivo MRI applications. J Mater Chem 19:6274–6693. https://doi.org/10.1039/B902394A

Rah YC, Han EJ, Park S, Rhee J, Koun S, Park HC, Choi J (2018) In vivo assay of the potential gadolinium-induced toxicity for sensory hair cells using a zebrafish animal model. J Appl Toxicol 38:1398–1404. https://doi.org/10.1002/jat.3656

Ramalho J, Ramalho M, Jay M, Burke LM, Semelka RC (2016) Gadolinium toxicity and treatment. Magn Reson Imaging 34: 1394–1398. https://doi.org/10.1016/j.mri.2016.09.005

Raschzok N, Langer CM, Schmidt C, Lerche KH, Billecke N, Nehls K, Schlüter NB, Leder A, Rohn S, Mogl MT, Lüdemann L, Stelter L, Teichgräber UK, Neuhaus P, Sauer IM (2013) Functionalizable silica-based micron-sized iron oxide particles for cellular magnetic resonance imaging. Cell Transplant 22:1959–1970. https://doi.org/10.3727/096368912X661382

Reddy AM, Kwak BK, Shim HJ, Ahn C, Lee HS, Suh YJ, Park ES (2010) In vivo tracking of mesenchymal stem cells labeled with a novel chitosan-coated superparamagnetic iron oxide nanoparticles using 3.0 T MRI. J Korean Med Sci 25:211–219. https://doi.org/10.3346/jkms.2010.25.2.211

Rogosnitzky M, Branch S (2016) Gadolinium-based contrast agent toxicity: a review of known and proposed mechanisms. Biometals 29:365–376. https://doi.org/10.1007/s10534-016-9931-7

Rohani P, Banerjee S, Sharifi-Asl S, Malekzadeh M, Shahbazian-Yassar R, Billinge SJ, Swihart MT (2019) Synthesis and

properties of plasmonic boron-hyperdoped silicon nanoparticles. Adv Funct Mater 29:1807788. https://doi.org/10.1002/adfm.201807788

Roth HC, Schwaminger SP, Schindler M, Wagner FE, Berensmeier S (2015) Influencing factors in the Co-precipitation process of superparamagnetic iron oxide nano particles: a model based study. J Magn Magn Mater 377:81–89. https://doi.org/10.1016/j.jmmm.2014.10.074

Saddik D, Troupis J, Tirman P, O'Donnell J, Howells R (2006) Prevalence and location of acetabular sublabral sulci at hip arthroscopy with retrospective MRI review. Am J Roentgenol 187:507–511. https://doi.org/10.2214/AJR.05.1465

Salazar-Alvarez G, Muhammed M, Zagorodni AA (2006) Novel flow injection synthesis of iron oxide nanoparticles with narrow size distribution. Chem Eng Sci 61:4625–4633. https://doi.org/10.1016/j.ces.2006.02.032

Sandiford L, Phinikaridou A, Protti A, Meszaros LK, Cui X, Yan Y, Frodsham G, Williamson PA, Gaddum N, Botnar RM, Blower PJ, Green MA, de Rosales RTM (2013) Bisphosphonate-anchored PEGylation and radiolabeling of superparamagnetic iron oxide: long-circulating nanoparticles for in vivo multimodal (T1 MRI-SPECT) imaging. ACS Nano 7:500–512. https://doi.org/10.1021/nn3046055

Sanjai C, Kothan S, Gonil P, Saesoo S, Sajomsang W (2014) Chitosan-triphosphate nanoparticles for encapsulation of super-paramagnetic iron oxide as an MRI contrast agent. Carbohydr Polym 104:231–237. https://doi.org/10.1016/j.carbpol.2014.01.012

Santra S, Kaittanis C, Grimm J, Perez JM (2009) Drug/dye-loaded, multifunctional iron oxide nanoparticles for combined targeted cancer therapy and dual optical/magnetic resonance imaging. Small 5:1862–1868. https://doi.org/10.1002/smll.200900389

Saraswathy A, Nazeer SS, Nimi N, Arumugam S, Shenoy SJ, Jayasree RS (2014) Synthesis and characterization of dextran stabilized superparamagnetic iron oxide nanoparticles for in vivo MR imaging of liver fibrosis. Carbohydr Polym 101:760–768. https://doi.org/10.1016/j.carbpol.2013.10.015

Sato N, Kobayashi H, Hiraga A, Saga T, Togashi K, Konishi J, Brechbiel MW (2001) Pharmacokinetics and enhancement patterns of macromolecular MR contrast agents with various sizes of polyamidoamine dendrimer cores. Magn Reson Med 46:1169–1173. https://doi.org/10.1002/mrm.1314

Sciancalepore C, Gualtieri AF, Scardi P, Flor A, Allia P, Tiberto P, Barrera G, Messori M, Bondioli F (2018) Structural characterization and functional correlation of Fe_3O_4 nanocrystals obtained using 2-ethyl-1, 3-hexanediol as innovative reactive solvent in non-hydrolytic sol-gel synthesis. Mater Chem Phys 207:337–349. https://doi.org/10.1016/j.matchemphys.2017.12.089

Shen F, Poncet-Legrand C, Somers S, Slade A, Yip C, Duft AM, Winnik F, Chang PL (2003) Properties of a novel magnetized alginate for magnetic resonance imaging. Biotechnol Bioeng 83:282–292. https://doi.org/10.1002/bit.10674

Shen CR, Wu ST, Tsai ZT, Wang JJ, Yen TC, Tsai JS, Shih M-F, Liu CL (2011) Characterization of quaternized chitosan-stabilized iron oxide nanoparticles as a novel potential magnetic resonance imaging contrast agent for cell tracking. Polym Int 60:945–950. https://doi.org/10.1002/pi.3059

Shi X, Wang SH, Swanson SD, Ge S, Cao Z, van Antwerp ME, Landmark KJ, Baker JR (2008a) Dendrimer-functionalized shell-crosslinked iron oxide nanoparticles for in-vivo magnetic resonance imaging of tumors. Adv Mater 20:1671–1678. https://doi.org/10.1002/adma.200702770

Shi Z, Neoh KG, Kang ET, Shuter B, Wang SC, Poh C, Wang W (2008b) (Carboxymethyl) chitosan-modified superparamagnetic iron oxide nanoparticles for magnetic resonance imaging of stem cells. ACS Appl Mater Interfaces 1:328–335. https://doi.org/10.1021/am8000538

Silva MF, de Oliveira LA, Ciciliati MA, Lima MK, Ivashita FF, de Oliveira DMF, Hechenleitner AAW, Pineda EA (2017) The effects and role of polyvinylpyrrolidone on the size and phase composition of iron oxide nanoparticles prepared by a modified sol-gel method. J Nanomater 2017:1–10. https://doi.org/10.1155/2017/7939727

Sodipo BK, Aziz AA (2018) One minute synthesis of aminosilane functionalized superparamagnetic iron oxide nanoparticles by sonochemical method. Ultrason Sonochem 40:837–840. https://doi.org/10.1016/j.ultsonch.2017.08.040

Spandonis Y, Heese FP, Hall LD (2004) High resolution MRI relaxation measurements of water in the articular cartilage of the meniscectomized rat knee at 4.7 T. Magn Reson Imaging 22:943–951. https://doi.org/10.1016/j.mri.2004.02.010

Stepanov A, Fedorenko S, Amirov R, Nizameev I, Kholin K, Voloshina A, Sapunova A, Mendes R, Rümmeli M, Gemming T, Mustafina A, Odintsov B (2018) Silica-coated iron-oxide nanoparticles doped with Gd (III) complexes as potential double contrast agents for magnetic resonance imaging at different field strengths. J Chem Sci 130:125–130. https://doi.org/10.1007/s12039-018-1527-z

Strable E, Bulte JWM, Moskowitz B, Vivekanandan K, Allen M, Douglas T (2001) Synthesis and characterization of soluble iron oxide-dendrimer composites. Chem Mater 13:2201–2209. https://doi.org/10.1021/cm010125i

Sun W, Mignani S, Shen M, Shi X (2016) Dendrimer-based magnetic iron oxide nanoparticles: their synthesis and biomedical applications. Drug Discovery Today 21:1873–1885. https://doi.org/10.1016/j.drudis.2016.06.028

Suryawanshi PL, Sonawane SH, Bhanvase BA, Ashokkumar M, Pimplapure MS, Gogate PR (2018) Synthesis of iron oxide nanoparticles in a continuous flow spiral microreactor and Corning® advanced flow™ reactor. Green Proc Syn 7:1–11. https://doi.org/10.1515/gps-2016-0138

Šutk A, Lagzdina S, Käämbre T, Pärna R, Kisandb V, Kleperis J, Maiorov M, Kikas A, Kuusik I, Jakovlevs D (2015) Study of the structural phase transformation of iron oxide nanoparticles from an Fe^{2+} ion source by precipitation under various synthesis parameters and temperatures. Mater Chem Phys 149–150:473–479. https://doi.org/10.1016/j.matchemphys.2014.10.048

Takami S, Sato T, Mousavand T, Ohara S, Umetsu M, Adschiri T (2007) Hydrothermal synthesis of surface-modified iron oxide nanoparticles. Mate Lett 61:4769–4772. https://doi.org/10.1016/j.matlet.2007.03.024

Teja AS, Koh PY (2009) Synthesis, properties, and applications of magnetic iron oxide nanoparticles. Prog Cryst Growth Charact Mater 55:22–45. https://doi.org/10.1016/j.pcrysgrow.2008.08.003

Thapa B, Diaz-Diestra D, Beltran-Huarac J, Weiner BR, Morell G (2017) Enhanced MRI T2 relaxivity in contrast-probed

anchor-free PEGylated iron oxide nanoparticles. Nanoscale Res Lett 12:312–325. https://doi.org/10.1186/s11671-017-2084-y

Thomson CE, Kornegay JN, Burn RA, Drayer BP, Hadley DM, Levesque DC, Gainsburg LA, Lane SB, Sharp NJ, Wheeler SJ (1993) Magnetic resonance imaging-a general overview of principles and examples in veterinary neurodiagnosis. Vet Radiol Ultrasound 34:2–17. https://doi.org/10.1111/j.1740-8261.1993.tb01986.x

Tian Q, Wang Q, Yao KX, Teng B, Zhang J, Yang S, Han Y (2014) Multifunctional polypyrrole@ Fe_3O_4 nanoparticles for dual-modal imaging and in vivo photothermal cancer therapy. Small 10:1063–1068. https://doi.org/10.1002/smll.201302042

Tromsdorf UI, Bruns OT, Salmen SC, Beisiegel U, Weller H (2009) A highly effective, nontoxic T1 MR contrast agent based on ultrasmall PEGylated iron oxide nanoparticles. Nano Lett 12:4434–4440. https://doi.org/10.1021/nl902715v

Tsai Z-T, Wang J-F, Kuo H-Y, Shen C-R, Wang J-J, Yen T-C (2010) In situ preparation of high relaxivity iron oxide nanoparticles by coating with chitosan: a potential MRI contrast agent useful for cell tracking. J Magn Magn Mater 322:208–213. https://doi.org/10.1016/j.jmmm.2009.08.049

Wang SH, Shi X, van Antwerp M, Cao Z, Swanson SD, Bi X, Baker JR (2007) Dendrimer-functionalized iron oxide nanoparticles for specific targeting and imaging of cancer cells. Adv Funct Mater 17:3043–3050. https://doi.org/10.1002/adfm.200601139

Wang L, Neoh KG, Kang ET, Shuter B, Wang SC (2009) Superparamagnetic hyperbranched polyglycerol-grafted Fe_3O_4 nanoparticles as a novel magnetic resonance imaging contrast agent: an in vitro assessment. Adv Funct Mater 19:2615–2622. https://doi.org/10.1002/adfm.200801689

Wang C, Ravi S, Garapati US, Das M, Howell M, Mallela J, Alwarapan S, Mohapatra SS, Mohapatra S (2013) Multifunctional chitosan magnetic-graphene (CMG) nanoparticles: a theranostic platform for tumor-targeted co-delivery of drugs, genes and MRI contrast agents. J Mater Chem B 1:4396–4405. https://doi.org/10.1039/C3TB20452A

Wang YXJ, Zhu XM, Liang Q, Cheng CH, Wang W, Leung KCF (2014) In vivo chemoembolization and magnetic resonance imaging of liver tumors by using iron oxide nanoshell/doxorubicin/poly (vinyl alcohol) hybrid composites. Angew Chem 53:4812–4815. https://doi.org/10.1002/anie.201402144

Wei H, Bruns OT, Kaul MG, Hansen EC, Barch M, Wiśniowska A, Chen O, Chen Y, Li N, Okada S, Cordero JM (2017) Exceedingly small iron oxide nanoparticles as positive MRI contrast agents. Proc Natl Acad Sci 114:2325–2330. https://doi.org/10.1073/pnas.1620145114

Winter JD, Akens MK, Cheng HLM (2011) Quantitative MRI assessment of VX2 tumour oxygenation changes in response to hyperoxia and hypercapnia. Phys Med Biol 5:1225–1229. https://doi.org/10.1088/0031-9155/56/5/001

Xiao Y, Lin ZT, Chen Y, Wang H, Deng YL, Le DE, Bin J, Li M, Liao Y, Liu Y, Bin J, Jiang G (2015) High molecular weight chitosan derivative polymeric micelles encapsulating superparamagnetic iron oxide for tumor-targeted magnetic resonance imaging. Int J Nanomed 10:1155–1172. https://doi.org/10.2147/IJN.S70022

Xiao YD, Paudel R, Liu J, Ma C, Zhang ZS, Zhou SK (2016) MRI contrast agents: classification and application. Int J Mol Med 38:1319–1326. https://doi.org/10.3892/ijmm.2016.2744

Xiong F, Hu K, Yu H, Zhou L, Song L, Zhang Y, Shan X, Liu J, Gu N (2017) A functional iron oxide nanoparticles modified with PLA-PEG-DG as tumor-targeted MRI contrast agent. Pharm Res 34:1683–1692. https://doi.org/10.1007/s11095-017-2165-8

Xu S, Yang F, Zhou X, Zhuang Y, Liu B, Mu Y, Wang X, Shen H, Zhi G, Wu D (2015) Uniform PEGylated PLGA microcapsules with embedded Fe_3O_4 nanoparticles for US/MR dual-modality imaging. ACS Appl Mater Interfaces 7:20460–20468. https://doi.org/10.1021/acsami.5b06594

Xue S, Wang Y, Wang M, Zhang L, Du X, Gu H, Zhang C (2014) Iodinated oil-loaded, fluorescent mesoporous silica-coated iron oxide nanoparticles for magnetic resonance imaging/computed tomography/fluorescence trimodal imaging. Int J Nanomed 9:2527–2538. https://doi.org/10.2147/IJN.S59754

Yadav RS, Kuřitka I, Vilcakova J, Jamatia T, Machovsky M, Skoda D, Urbánek P, Masař M, Urbánek M, Kalina L, Havlica J (2020) Impact of sonochemical synthesis condition on the structural and physical properties of $MnFe_2O_4$ spinel ferrite nanoparticles. Ultrason Sonochem 61:104839. https://doi.org/10.1016/j.ultsonch.2019.104839

Yamada Y, Shimizu R, Kobayashi Y (2016) Iron oxide and iron carbide particles produced by the polyol method. Hyperfine Interact 237:6–11. https://doi.org/10.1007/s10751-016-1220-x

Yan F, Xu H, Anker J, Kopelman R, Ross B, Rehemtulla A, Reddy R (2004) Synthesis and characterization of silica-embedded iron oxide nanoparticles for magnetic resonance imaging. J Nanosci Nanotechnol 4:72–76. https://doi.org/10.1166/jnn.2004.074

Yang QX, Wang J, Collins CM, Smith MB, Zhang X, Ugurbil K, Chen W (2004) Phantom design method for high-field MRI human systems. Magn Reson Med 52:1016–1020. https://doi.org/10.1002/mrm.20245

Ye F, Laurent S, Fornara A, Astolfi L, Qin J, Roch A, Martini A, Toprak MS, Muller RN, Muhammed M (2012) Uniform mesoporous silica coated iron oxide nanoparticles as a highly efficient, nontoxic MRI T2 contrast agent with tunable proton relaxivities. Contrast Media Mol Imaging 7:460–468. https://doi.org/10.1002/cmmi.1473

Yue-Jian C, Juan T, Fei X, Jia-Bi Z, Ning G, Yi-Hua Z, Ye D, Liang G (2010) Synthesis, self-assembly, and characterization of PEG-coated iron oxide nanoparticles as potential MRI contrast agent. Drug Dev Ind Pharm 36:1235–1244. https://doi.org/10.3109/03639041003710151

Zhang C, Wängler B, Morgenstern B, Zentgraf H, Eisenhut M, Untenecker H, Krüger R, Huss R, Seliger C, Semmler W, Kiessling F (2007) Silica-and alkoxysilane-coated ultrasmall superparamagnetic iron oxide particles: a promising tool to label cells for magnetic resonance imaging. Langmuir 23:1427–1434. https://doi.org/10.1021/la061879k

Zhang Y, Liu JY, Ma S, Zhang YJ, Zhao X, Zhang XD, Zhang ZD (2010) Synthesis of PVP-coated ultra-small Fe_3 O_4 nanoparticles as a MRI contrast agent. J Mater Sci Mater Med 21:1205–1210. https://doi.org/10.1007/s10856-009-3881-3

Zheng X-C, Ren W, Zhang S, Zhong T, Duan X-C, Yin Y-F, Xu M-Q, Hao Y-L, Li Z-T, Li H, Liu M, Li Z-Y, Zhang X (2018) The theranostic efficiency of tumor-specific, pH-responsive,

peptide-modified, liposome-containing paclitaxel and superparamagnetic iron oxide nanoparticles. Int J Nanomed 13:1495–1504

Zhou C, Rong P, Zhang W, Zhou J, Zhang Q, Wang WEI, Zou B (2010) Fulvic acid coated iron oxide nanoparticles for magnetic resonance imaging contrast agent. Funct Mater Lett 3: 197–200. https://doi.org/10.1142/S179360471000124X

Zhou D, Sun Y, Zheng Y, Ran H, Li P, Wang Z, Wang Z (2015) Superparamagnetic PLGA–iron oxide microspheres as contrast agents for dual-imaging and the enhancement of the effects of high-intensity focused ultrasound ablation on liver tissue. RSC Adv 5:35693–35703. https://doi.org/10.1039/C5RA00880H